Quantifying bacterial evolution in the wild: a birthday problem for *Campylobacter* lineages

Jessica K. Calland[1], Ben Pascoe[1], Sion C. Bayliss[1], Evangelos Mourkas[1], Elvire Berthenet[2], Harry A. Thorpe[1], Matthew D. Hitchings[3], Edward J. Feil[1], Martin J. Blaser[4], Daniel Falush[5]# & Samuel K. Sheppard[1]#

[1]The Milner Centre for Evolution, University of Bath, Claverton down, Bath, UK; [2]French National Reference Center for Campylobacters and Helicobacters, University of Bordeaux, 33076, Bordeaux, France; [3]Institute of Life Sciences, Swansea University Medical School, Swansea University, Singleton Park, Swansea, UK; [4]Center for Advanced Biotechnology and Medicine, Rutgers University, New Brunswick, New Jersey, USA; [6]Centre for Microbes, Development and Health, Institute Pasteur Shanghai, China.

#Authors to which correspondence should be addressed: s.k.sheppard@bath.ac.uk & daniel.falush@ips.ac.cn

Short title: *Campylobacter* molecular clock

Keywords: Evolution / Pathogenesis / Molecular clock / Population structure / Population genomics.

Abstract

Measuring molecular evolution in bacteria typically requires estimation of the rate at which nucleotide changes accumulate in strains sampled at different times that share a common ancestor. This approach has been useful for dating ecological and evolutionary events that coincide with the emergence of important lineages, such as outbreak strains and obligate human pathogens. However, in multi-host (niche) transmission scenarios, where the pathogen is essentially an opportunistic environmental organism, sampling is often sporadic and rarely reflects the overall population, particularly when concentrated on clinical isolates. This means that approaches that assume recent common ancestry are not applicable. Here we present a new approach to estimate the molecular clock rate in *Campylobacter* that draws on the popular probability conundrum known as the 'birthday problem'. Using large genomic datasets and comparative genomic approaches, we use isolate pairs that share recent common ancestry to estimate the rate of nucleotide change for the population. Identifying synonymous and non-synonymous nucleotide changes, both within and outside of recombined regions of the genome, we quantify clock-like diversification to estimate synonymous rates of nucleotide change for the common pathogenic bacteria *Campylobacter coli* (2.4×10^{-6} s/s/y) and *Campylobacter jejuni* (3.4×10^{-6} s/s/y). Finally, using estimated total rates of nucleotide change, we infer the number of effective lineages within the sample time-frame – analogous to a shared birthdays – and assess the rate of turnover of lineages in our sample set over short evolutionary timescales. This provides a generalizable approach to calibrating rates in populations of environmental bacteria and shows that multiple lineages are maintained, implying that large-scale clonal sweeps may take hundreds of years or more in these species.

Author Summary

Growth and reproduction in living organisms require DNA replication but this process is error prone. Along with variation introduced by horizontal gene transfer, it can lead to alterations in the nucleotide sequence. These nucleotide changes accumulate over time in successive generations at an approximately constant rate termed the molecular clock. Therefore, if this rate is known, one can estimate the date when two or more lineages diverged. In bacteria, this can be informative for understanding the time-scale of emergence and spread of pathogenic strains. Such analyses are robust when the ancestral population is known, such as for obligate pathogens that only infect humans. However, when the bacterium inhabits multiple hosts or niches it is difficult to infer direct ancestry from one strain to another, reducing the accuracy of molecular clock estimates. Here we focus on one such multi-host organism, *Campylobacter*, a leading cause of food-borne gastroenteritis. Reconstructing the population history by estimating empirical nucleotide change rates from carefully selected isolate pairs, and evaluating the maintenance of multiple lineages over time, we provide information about strain diversification. Our method is a new addition to the bacterial genomics toolkit that will help in understanding the spread of opportunistic pathogens.

Introduction

Theoretical models of a relatively constant rate of molecular change over time [1], the molecular clock, have become fundamental to explaining the evolution in bacteria [2,3]. Spurred by the increasing availability of population-scale genome datasets, it is now common for comparative genomic studies to describe not only the relatedness of isolates but also how long ago they diverged [4-8]. This can provide valuable information when combined with host,

habitat or ecosystem data. For example, it is possible to investigate how events such as host transitions or global dissemination have influenced the emergence and spread of lineages that may display important phenotypes, including pathogenicity.

There are significant challenges when applying molecular clocks to date lineage diversification in natural bacterial populations. In particular, it is necessary to determine the rate at which the clock 'ticks' and the uniform accumulation of nucleotide change (NC) over time. However, this is not simply a reflection of the background point mutation rate (associated with replication error) and the generation time of the bacterium [9,10], but is also influenced by horizontal gene transfer (HGT) that can introduce several NCs in a single event [11]. Furthermore, the rate at which NCs accumulate in the population is influenced by the population size [12] and selection (positive and stabilizing) on different fitness effects [13].

While debate continues about NCs that are effectively neutral, and hence provide accurate clock estimates [14], there is clear utility for even approximations of the rate of genome change over time [15,16]. This has allowed the development of time-calibrated phylogenies explaining molecular evolution in numerous well-known pathogen species [4-7]. However, even with large genome datasets and increasingly sophisticated models [17,18], the accuracy of molecular evolution estimates is dependent upon the data from which they are derived, and two important considerations remain. First, the data should represent a longitudinal sample set [15,19]. Second, the data should be representative of the population as a whole.

It is conceptually simple to understand how a long time-frame between collection of the earliest and latest sample would increase the number of NCs recorded, and how sampling at consistent

intervals could help to determine if accumulation was linear over time. Comparisons between modern samples and DNA from the stomach of a 5,300 year old frozen iceman 'Otzi' have been used to investigate the emergence of modern *Helicobacter pylori* lineages [20]. However, ancient pathogen samples are rarely available. More frequently, molecular clock rates are estimated using collections of contemporary isolates that often share a common ancestor older than the sample frame. Convincing estimations have been possible for medically important bacteria, through comparison of large numbers of closely related isolates [21-24] but for many pathogens sampling of outbreaks may not provide an adequate representation of the bacterial population.

Most disease-causing bacteria are not obligate human pathogens. In this case, large reservoirs of isolates from which infection can arise may be infrequently sampled, despite their potential importance as emergent pathogenic strains. For example, *Campylobacter jejuni* and *C. coli* are among the most common causes of bacterial gastroenteritis worldwide but exist principally as commensal organisms in the gut of mammals and birds [25-29]. Human infection results primarily via food contaminated with strains from wild and agricultural animals, especially chickens [30-35]. In multi-host (niche) transmission scenarios such as this, where the pathogen is essentially an environmental organism, sampling is often sporadic and rarely reflects the overall population, particularly when concentrated on clinical isolates [36].

Overcoming the problem of sporadic or unrepresentative sampling for molecular clock estimation requires that sufficient numbers of isolates are collected to ensure that there are pairs that share a recent common ancestor (within the sampling period). However, with the enormous effective population size of environmental bacteria populations, questions remain about how

many isolates need to be sampled to achieve this. This is analogous to the well-known probability theory conundrum known as the birthday problem [37]. This puzzle asks how many randomly chosen people need to be sampled so that a pair of them will share the same birthday. To be sure, requires a sample size of 366 (the number of possible birthdays), assuming that all birthdays are equally common, but a 99.9% probability is achieved with just 70 people and 50% with 23 people. This may seem counter intuitive but can be explained by considering that rather than comparing the birthday of a single individual to everyone else's, in fact comparisons are made between every pair of individuals, 23 x 22/2 = 253. The result is greater than half the number days in the year, hence the 50% probability. Clearly, there are challenges in relating this conceptual model to bacteria. First, it is not known how many possible lineages (here equivalent to birthdays) there are in natural bacterial populations. Second, how to define lineages or isolate pairs with recent common ancestry. Third, just as with birthdays, some lineages are far more common than others. For example, of >72,000 *C. jejuni* and *C. coli* isolates archived in the pubMLST database [38], >50% belong to just 5 clonal complexes (out of 45).

Together, factors relating to isolate sampling and genome analysis conspire such that it may be difficult to distinguish NCs that reflect the passage of time [16,39]. Here, we take a multi-layered approach to estimate the rate of molecular evolution of *C. jejuni* and *C. coli* using a large genome collection (2,425 genomes) representing isolates sampled over a 46-year period. We begin by identifying closely related isolate pairs in which the most recently sampled isolate has accumulated NCs over time. We then quantify synonymous and non-synonymous polymorphisms to take (some) account of selection, both within and outside of recombinant regions of the genome, and use synonymous polymorphisms to quantify clock-like

diversification in *Campylobacter* [40,41]. Finally, using estimated rates of nucleotide change we assess the rate of turnover of lineages in our sample sets over short evolutionary timescales. This provides a generalizable approach to calibrating rates in populations of environmental bacteria and clues about lineage diversification in two important enteric pathogens.

Results

There is a weak temporal signal in *C. coli* and *C. jejuni* phylogenies

Core genome phylogenies revealed little evidence of clustering by collection date (**Fig 1**). Isolates belonging to common sequence types (STs) and clonal complexes were sampled over the 46-year period. These included poultry associated ST-353, ST-354 and ST-257 complexes, cattle associated ST-61 and ST-42 complexes, and host generalist ST-21, ST-45, ST-828 (*C. coli*) complexes [42] (**Fig 1 and S1 Table**). Linear regression of root-to-tip distances and sampling dates of *C. coli* and *C. jejuni* phylogenies **(S1 and S2 Fig)**, using TempEst software, provided very weak evidence of a temporal signal when the best-fitting root was estimated. The R^2 values were low for both *C. coli* ($R^2 = 0.176$, slope = 3×10^{-5}) and *C. jejuni* ($R^2 = 9.5 \times 10^{-2}$, slope = 6.4×10^{-5}) phylogenies (**S2 and S3 Tables**). Consistent with some other studies [43], this poor branch-length to isolation date correlation suggests that estimation of the molecular clock rate from the entire dataset may be difficult. However, the accumulation of polymorphisms exhibited a positive correlation with sampling date in all datasets (**S1 and S2 Figs**) implying the maintenance of multiple STs and clonal complexes through time.

Analyses of temporal signal can be improved in bacterial genomes by the removal of recombined regions where multiple genetic variations may be introduced in a single

evolutionary event [44]. Masking recombination in this way is challenging for large genome datasets such as those used in this study. Therefore, we conducted root-to-tip regression analysis on sub-lineages within *C. coli* and *C. jejuni* where recombination events could be efficiently excluded (**S2 and S3 Tables**). Consistent with previous studies [44], any lineage with an R^2 value >0.5 was described as having a strong temporal signal and was used in subsequent Bayesian evolutionary analysis. There were large differences in the strength of the temporal signal across all sub-lineages with the lowest R^2 value found in the host generalist *C. jejuni* ST-45 clonal complex (R^2 = 0.0229, slope = 1.89 x 10^{-5}) and highest in *C. coli* ST-1090 (R^2 = 0.8603, slope = 7.07 x 10^{-5}) (**S2 and S3 Tables**). However, only 3 out of 8 *C. coli* and 5 out of 18 *C. jejuni* sub-lineages exhibited strong temporal signal with R^2 >0.5.

Bayesian evolutionary analyses were performed on sub-lineages where temporal signal was strong (R^2 > 0.5) using BEAST2 [45]. This excluded species-wide datasets but included 3 *C. coli* and 5 *C. jejuni* sub-lineages for which rate estimates were obtained (**S2 and S3 Tables**). Mean rate estimates were similar for all 3 *C. coli* lineages averaging at 7.82 x 10^{-4} s/s/y but varied from 8.20 x 10^{-5} (ST-661 clonal complex) to 1.00 x 10^{-3} s/s/y (ST-22 clonal complex) for *C. jejuni* (**S2 and S3 Tables**). In part because of the poor temporal signal in the species-wide analyses and most sub-lineages, we developed an alternative method using paired isolates.

Sampling matched isolate pairs allows estimation of the rate of nucleotide change

Nucleotide change (NC) is introduced into the bacterial genome by recombination resulting from HGT and point mutation. For clarification, we use the empirical term ‘nucleotide change’ to describe any nucleotide variation resulting from these two processes, consistent with previous studies [46]. Estimation of molecular clock rates requires comparison of isolates from

related, or preferably the same, lineages that have accumulated NCs over time. To achieve this there is a necessary balance between maximizing the time between sampling and accumulated NCs whilst ensuring comparisons are made between related strains. Therefore, we plotted NC difference against time difference to determine criteria for choosing comparable isolate pairs (**Fig 2**). The sample time difference was chosen to maximize the time between sampling and the number of comparable pairs belonging to the same lineage. Pair selection criteria were standardised for both species so that isolate pairs were included where the sampling time difference was >8 years and there were <5000 SNPs between them (**Fig 2, S4 Table, Tables 1 and 2**). Based upon these criteria, there were 18 *C. coli* and 74 *C. jejuni* isolate pairs (**S4 Table**). However, for consistency between the species we chose the 20 *C. jejuni* pairs with the highest nucleotide identity, hence those with the strongest evidence of recent common ancestry. Therefore 18 *C. coli* and 20 *C. jejuni* pairs comprised the dataset for NC rate calibration. These belonged to the ST-21, ST-22, ST-45, ST-1332, ST-828 clonal complexes and isolate pairs had a difference in sampling date of 8 to 11 years (*C. coli*) and 8 to 36 years (*C. jejuni*) (**Tables 1 and 2, S4 Table**).

Estimation of a molecular clock rate requires that NCs accumulate over time, defined here as NCs per site per year (s/s/y). It is also possible that branch shortening can occur where there are fewer NCs in the more recent isolate of a pair. While not specifically describing branch shortening, negative rates of NC have previously been observed [44. In this study, 13 out 18 *C. coli* and 11 out of 20 *C. jejuni* isolate pairs exhibited branch lengthening, that is to say more total NCs (within and outside recombined regions) were found in the more recent isolate (**Tables 3 and 4, S5 Table**). Only pairs having undergone measurable evolution (branch lengthening) were included in further analysis of the accumulation of NCs over time. While

this may inflate our estimate of the NC rate, it was necessary to ensure a positive rate for calculating the number of effective lineages. For measurably evolving isolate pairs, the total NC rate was calculated as well as the rates within and outside of recombined regions (**Table 5, S6 Table**). The mean NC rate for non-recombined regions was 6.36 x 10^{-6} and 8.45 x 10^{-6} s/s/y but ranged from 1.60 x 10^{-6} – 1.50 x 10^{-6} and 1.00 x 10^{-7} – 3.60 x 10^{-5} s/s/y for *C. coli* and *C. jejuni* respectively, or 11.46 and 13.53 average NCs per genome per year (s/g/y) (**Table 5**).

Recombination drives molecular evolution in *Campylobacter*

NCs in coding sequence based on gene definitions in the reference *C. coli* (YH501) and *C. jejuni* (NCTC 11168) isolate genomes introduced an average of 1569 and 242 NCs in *C. coli* and *C. jejuni* paired genome datasets respectively. Of these, an average of only 222 (*C. coli*) and 106 (*C. jejuni*) were inferred to be the result of point mutation, with the remainder resulting from recombination (**Tables 3 and 4**). Recombination is therefore the major source of sequence variation in both species (**Fig 3, Tables 3 and 4**), introducing nearly six times as many NCs in *C. coli* than in *C. jejuni* – consistent with previous estimates based upon MLST [47]. To assess the effect of NCs on amino acid sequences we quantified non-synonymous (N) and synonymous (S) NCs and determined the ratio per site (*dN/dS*) for all isolate pairs in recombined and non-recombined sequence (**Tables 3 and 4**). Point mutation accounted for an unequal amount of N and S polymorphism both within and between species (*C. coli*, N = 99, S = 123; *C. jejuni*, N = 63, S = 43). While recombination introduced many more NCs than point mutation, in both species these were biased towards synonymous changes. Specifically, around six times as many S than N NCs were introduced by recombination in *C. coli* and approximately twice more in *C. jejuni* (*C. coli*, N = 546, S = 801; *C. jejuni*, N = 59, S = 77). Overall, average *dN/dS* ratios were consistent between species within recombined (*C. coli* 0.492, *C. jejuni* 0.490) and non-

recombined (*C. coli* 0.594, *C. jejuni* 0.509) portions of the genome. However, because of the relative importance of recombination (*r/m* = 37.240 (*C. coli*), *r/m* = 5.098 (*C. jejuni*)), on average N NCs were similar for *C. jejuni* from recombination and point mutation (59 and 63 respectively). However, recombination introduced 5.5 times more N NCs than point mutation in *C. coli* (**Tables 3 and 4**). Variation in *dN/dS* was observed between isolate pairs but was mostly indicative of purifying selection (*dN/dS*<1). Evidence of positive selection (*dN/dS*>1) was only observed within recombined sequence in 6 isolate pairs (**Tables 3 and 4**). It is important to note that, while *dN/dS* comparisons have been made between closely related bacteria within the same species [48,49], this method was originally intended for between species comparisons [50].

Additional analysis of the distribution of recombination events revealed that an average of 13% (*C. coli*) and 2% (*C. jejuni*) of the genome has undergone recombination in at least one isolate pair since divergence from the common ancestor of each sub-tree (**Tables 6 and 7**). Recombination was distributed across the genome in both species but was elevated in certain regions of *C. coli* introducing more NCs at potential recombination hotspots [51]. However, recombination remained the main source of variation in both species (**Fig 3**).

Molecular clock estimates for *C. coli* and *C. jejuni*

Molecular clock estimates require that NCs accumulate at a consistent rate over time. We maximized the chance of identifying this signal in several ways. First, genomic variation within recombined regions was discounted as multiple NCs can be introduced in a single evolutionary event – distorting clock estimates [39,47,52]. Second, non-synonymous NCs were discounted as selection may be more likely to influence the frequency of variation at these sites. Third,

only pairs in which the most recently sampled isolate contained more NCs (branch lengthening) were used as they displayed measurable evolution over time. Based on these criteria, a similar average molecular clock rate was obtained for *C. coli*, 2.4 x 10^{-6} s/s/y (4.27 s/g/y), and *C. jejuni*, 3.4 x 10^{-6} s/s/y (5.42 s/g/y) (**Table 5**) but ranged from 2.1 x 10^{-7} – 7.7 x 10^{-6} and 3.8 x 10^{-8} – 1.7 x 10^{-5} s/s/y.

Coalescence and maintenance of lineages over time

Molecular clock estimates can vary within a population. Therefore the applicability of generalized clocks depend upon how much of the population has been sampled. To quantify this we estimated the average total NC rate (***μ***) (*C. coli* = 77.292 s/g/y, *C. jejuni* = 14.101 s/g/y), including all NCs within and outside recombined sequence. These rates were used to determine the number of coalescences in the population at a given time point (here referred to as '*effective lineages'*) within the dataset. The maximum timeframe for comparison was 37 years for *C. coli* and 46 years for *C. jejuni* (short in evolutionary terms). This provided information about the number of ancestral strains and the rate of turnover of lineages within the dataset. The total number of potential pairs without accounting for genetic similarity (***Y***), was equal to the square of the total number of isolates (n^2) divided by two (to avoid double counting of isolate pairs), 180,600 and 1,663,488 for *C. coli* and *C. jejuni* respectively.

Having determined the total NC rate, we were able to predict the expected number of NCs over a given period of time. For example, 14 in 1 year for *C. jejuni*. We then subsampled all isolate pairs (***Y***) to determine how many isolate pairs had $\leq$14 NCs between them – 76 isolate pairs. This is the possible number of isolate pairs that have arisen in 1 year. This process was repeated for each time cut-off, up to a maximum of 37 and 46 years for *C. coli* and *C. jejuni* respectively

(**Tables 8 and 9**), to give the number of possible pairs for every time cut-off (***X***) (**Figs 2B and 2D**). Dividing ***Y/X*** resulted in the number of coalescences (*effective lineages*) at a given time interval in the past (***Z***) (**Tables 8 and 9**). For example, if the total NC rate was 14 s/g/y and we were interested in the number of birthdays within 5 years of our dataset, we would multiply the NC rate by 5 to result in 70 NCs of evolution over 5 years. The number of *potential pairs* (***Y*** = 1,663,488) / *possible pairs* (***X*** = 174) = ~9,560 coalescences (ancestors) within this time period (**S3 Fig**, **Tables 8 and 9**).

The number of effective lineages at a given time-point can also be interpreted as the number of lineages that gave rise to those that are seen today. This provides valuable information about how the population is maintained over time and the extent to which it has diversified. For example, 1,263 *C. coli* lineages 37 years ago gave rise to an estimated 22,575 one year ago and 4,726 *C. jejuni* lineages 46 years ago gave rise to 21,888 lineages one year ago. This equates to an average increase in the number of effective lineages of 576 and 373 per year for *C. coli* and *C. jejuni* respectively. For *C. jejuni* it is clear that a considerable proportion (22%) of all lineages have been maintained throughout the 46 year sampling period and probably much longer (**Fig 4**). In contrast, only 6% of all effective lineages were present in the *C. coli* population 37 years ago. Perhaps the most striking finding is that the *C. coli* population has rapidly diversified in recent years. For example, there has been an 800% increase in the number of effective lineages in the last 10 years, over 3 times the rate of increase observed in *C. jejuni* (**Fig 4, S3 Fig**).

Discussion

The increasing availability of large genome datasets has great potential for improving molecular clock estimates in bacteria. However, significant challenges remain. While it is clear that the frequency of NCs can vary between different species and strains [6,7,10,24,44,53,54], the extent to which nucleotide variation represents an intrinsic molecular clock is often less apparent. Biological factors such as generation time, population size and recombination rate, and ecological factors including cellular responses to habitat variation or stress and the strength of natural selection, influence the rate at which NCs accumulate in populations [55]. Therefore, obtaining a robust molecular clock estimate from natural bacterial populations requires an appropriate sample frame and careful consideration of the nature of observed sequence variation.

In cases where there is a clear temporal signal among isolates, it may be possible to obtain a robust molecular clock estimate by applying models to large genome datasets [24]. However, analysing all *C. coli* and *C. jejuni* genomes gave a weak temporal signal. This is likely related to the population structure and biology of these organisms that is in stark contrast to many obligate human pathogens [24]. Consistent with many other zoonotic or environmental bacteria, *Campylobacter* is a diverse genus with multiple lineages (STs and clonal complexes) inhabiting multiple hosts/niches. This required a more targeted approach to microevolutionary analysis consistent with that used to investigate transmission in similarly variable organisms [21].

Sub-sampling within the isolate collection, sampled over 46 years, identified closely related pairs of isolates with divergent sampling dates. Clearly, calibration of the molecular clock requires that NCs accumulate over time. This was not the case in all isolate pairs. In some cases, the most recently sampled isolate had accumulated fewer NCs than the comparator strain

leading to a negative NC rate. A negative slope of the root-to-tip regression line has been interpreted as evidence for a lack of temporal signal or for a large dispersion of the rate of change [24,44]. Furthermore other studies have described the time-dependency of molecular evolution [56,57] and it can be the case that deleterious NCs in the older isolate have been purged leading to differences in long and short term molecular clock estimates [48,58]. To simplify interpretation in our study, isolate pairs where the most recent isolate had not accumulated NCs were excluded from the analysis. While this might inflate the NC rate estimate, in organisms with complex ecology such as *Campylobacter*, it is also possible that closely related isolates occupy different sub-niches and experience different selection pressures even when sampled from the same host.

Returning to the birthday problem analogy, considering the number of isolate pairs (equivalent to people with the same birthday) obtained from the original genome dataset can provide clues about the extent of lineage diversity in the natural population. Using total NC rates, we were able to assess the nature of coalescence across the sample time frame for each species. The coalescence we refer to here is equivalent to the number of ancestral strains at a particular time point (effective lineages) in the natural environment from which contemporary strains emerged. Effective population size (Ne) is commonly used to reflect the number of individuals in a population that contribute to subsequent generations [59]. This has been used to investigate bacteria but contrasting approaches can provide different estimates depending on the method used [53,60]. The idea of effective lineages, described in this study, is related to Ne but is more specific for organisms that reproduce clonally. Rather than typical Ne estimates for sexual populations, where the mating of two individuals is largely independent of what happened in previous generations, the number of effective lineages in a bacterial population reflects the

number of distinct lineages that will survive and therefore contribute to future generations. This provides information on the genetic inertia of the population.

These analyses highlighted the importance of appropriate sampling when calibrating NC rates and can help in determining the extent to which samples represent the population as a whole. Specifically, by considering the number of coalescences in a random population, we can look back through the sample time frame to estimate the number of effective lineages across a randomly sampled dataset. For example, suppose we would like to know if our contemporary isolates have a common ancestor in 1980. We know that a proportion of these ancestors gave rise to the diversity we see today but many lineages would go extinct and therefore not contribute [61]. Based on an average NC rate of 14 s/g/y for *C. jejuni*, there would be 560 NCs over 40 years total evolution between a strain pair. So, one can then ask how many pairs are close enough genetically for that to be the case. This gives an estimate of the effective number of ancestors in 1980 that gave rise to the contemporary dataset - equivalent to the number of birthdays.

Our estimate of effective lineages aims to better account for both unobserved lineages and lineages that co-exist over a long period of time. Both of these estimates are strongly affected by the sample frame and, while we have relatively large isolate collections from livestock and humans, the same cannot be said for the vast number of other potential host and environmental sources. Therefore, our estimate of effective lineages is more useful as an estimate of the number of ancestors that have given rise to the diversity of strains that we see today. For *Campylobacter*, it is clear that multiple lineages have persisted over a long period of time. This indicates that although the population is large, the strains are not turning over at a particularly

fast rate. The absence of lineage replacement is inconsistent with some models of bacterial evolution that predict periodic population bottlenecks [62] but this can be explained in several ways. First, it is possible that the 37/46 year sampling period in this study is not sufficient time to out-compete a rival strain. Second, bacteria occupy different niches that are sustained so strains are not in direct competition. Third, the fitness differences among strains are not great enough for one lineage to out-compete another.

As well as the maintenance of multiple lineages, there is also evidence for variation in the number of effective lineages that contributed to successive generations between the two major pathogenic *Campylobacter* species. While, demographic inference and estimates of the number of generations using BEAST were similar for *C. coli* and *C. jejuni* (**S2 and S3 Tables**), the number of effective lineages was shown to be consistently higher for *C. jejuni* throughout much of the sample frame. Furthermore, there was evidence for a rapid increase in the number of *C. coli* lineages that began around 8 years ago (**Fig 4**). The reason for this is unclear. The average synonymous NC rate estimates were similar for *C. jejuni* and *C. coli*, 3.4×10^{-6} and 2.4×10^{-6} s/s/y respectively, equating to approximately 5.4 (*C. jejuni*) and 4.3 (*C. coli*) NCs per genome per year. This is somewhat lower than previous estimates for *C. jejuni* calculated from 7-locus MLST (2.79×10^{-5} s/s/y) [47] but is within the range of molecular clock estimates calculated from genomic variation for *Enterococcus faecium* (9.35×10^{-6} s/s/y) and *Y. pestis* (1.57×10^{-8} s/s/y) [44]. Although average synonymous NC rates were consistent with other estimates, rates ranged from 2.10×10^{-7} to 7.70×10^{-6} s/s/y in *C. coli* and 3.80×10^{-8} to 1.70×10^{-5} s/s/y for *C. jejuni*. This implies uncertainty around the estimate. However, rate heterogeneity among lineages is not uncommon in bacterial species [63] potentially reflecting differences in the evolution and ecology of different species and strains.

While the average NC rate was consistent for *C. coli* and *C. jejuni*, the relative number of NCs introduced by homologous recombination and mutation (*r/m*) differed markedly, with on average 37-fold (*C. coli*), compared to 5-fold (*C. jejuni*), greater impact on sequence variation. HGT is known to be an important driver of genome evolution in *Campylobacter* [47,64] but these estimates are considerably higher than previous ones using 7-locus MLST [11]. Recombination introduced nearly twice as many synonymous than non-synonymous NCs, but even taking this into account, recombined sequence accounted for around 79% of all non-synonymous variation. This highlights the importance of HGT in rapidly evolving *Campylobacter* genomes and provides evidence that recombination may have been an important factor in the recent diversification of *C. coli* [26,65,66], potentially associated with an adaptive radiation [67,68] linked to the colonization of agricultural niches [69]. However, this should be balanced against the evidence of purifying selection within recombined sequence (*dN/dS* = 0.492 for *C. coli* and 0.49 for *C. jejuni)* and the removal of non-synonymous NCs through negative selection [48].

Finally, throughout this study we have emphasized the importance of sampling so that measures of molecular evolution are obtained by comparing recent samples with a true ancestor. The uneven distribution of lineages within the population and the possibility that they differ in key evolutionary measures (*r/m* and *dN/dS*), means that our molecular clock estimate may not be applicable to all *Campylobacter* lineages [21,71-72]. Perhaps this is best illustrated by considering two host-specialist *C. jejuni* lineages, one associated with chickens and the other with cattle [8,26]. There are 19 billion chickens on earth compared to 1.3 billion cattle [73] and *C. jejuni* colonizes up to 80% of chickens [74] with much lower rates in cattle. As the efficiency

by which natural selection acts on sequence variation is related to effective population size [41], the rate of fixation and removal of NCs will be much faster in *C. jejuni* in chickens. Furthermore, chickens have a higher body temperature than cattle therefore the *C. jejuni* will grow faster, have a shorter generation time, and accumulate NCs at a higher rate [9]. From this simple example, which ignores many important factors (eg. subniche structure, host transition bottle necking, resident microbiome) it is clear molecular evolution can be influenced by population-scale forces down to the physiology of the individual cell. The approach employed in this study goes some way towards mitigating effects that confound generalized molecular clock estimates. Focussing on well-defined closely related isolate pairs inevitably reduces the number of comparisons from which the mean molecular clock rate is estimated. However, consideration of the distribution of effective lineages within the population is essential for identifying robust molecular clock estimates in environmental bacteria with complex multi-host ecology and massive effective population sizes.

Materials and Methods

Isolate sampling, genome sequencing and assembly

The accuracy of molecular clock estimates are improved by analysing large numbers of isolates sampled over long time periods. While very large isolate genome collections exist for *Campylobacter* (see below), many of these were sampled within the last 20 years. Therefore, to extend the sample time frame we assembled an isolate collection comprising 53 isolates sampled between 1978 and 1985 (12 *C. coli*, 41 *C. jejuni*) derived from multiple sources (human, duck, cattle, dog, turkey, wild bird and pig (**S1 Table**)). These samples were streaked onto mCCDA (PO0119A Oxoid Ltd, Basingstoke, UK) with CCDA Selective Supplement

(SR0155E Oxoid Ltd, Basingstoke, UK) and incubated at 37˚C for 48h in a microaerobic atmosphere (85% N_2, 10% CO_2, and 5% O_2) using CampyGen Compact sachets (Thermo Fisher Scientific Oxoid Ltd, Basingstoke UK). Single colonies from each plate was then sub-cultured onto Mueller Hinton (MH) (CM0337 Oxoid Ltd, Basingstoke, UK) agar and grown for an additional 48h at 37˚C and stored in 20% glycerol stocks at -80˚C.

DNA was extracted using the QIAamp DNA Mini Kit (QIAGEN, Crawley, UK), according to manufacturer's instructions. DNA was quantified using a Nanodrop spectrophotometer before sequencing on an Illumina MiSeq sequencer using the Nextera XT library preparation kits with standard protocols. Paired end libraries were sequenced using 2 × 300 bp 3rd generation reagent kits (Illumina). Short read data was assembled using the *de novo* assembly algorithm, SPAdes (version 3.10.0 35) [75] generating an average of 49 contigs (range: 2 -115) for a total average assembled genome size of 1.69 Mbp (range: 1.62-1.80). The average N50 was 189,430 bp (range: 81,283-974,529). These isolate genomes were augmented with 1,783 *C. jejuni* and 589 *C. coli* genomes archived in BIGSdb [76] representing isolates sampled from multiple sources (human, cattle, chicken, cat, dog, duck, environmental waters, farm environments, geese, lamb, rabbit, sand, seal, wild birds, turkey, pig) between 1970 and 2016 (**S1 Table).** The total isolate collection comprised 2,425 *Campylobacter* genomes, including *C. jejuni* belonging to 286 STs and 36 clonal complexes, and *C. coli* to 125 STs and 1 clonal complex. All assembled genomes and raw reads have been deposited in the NCBI repository associated with BioProject: PRJNA524315. Individual accession numbers can be found in **S1 Table**. Assembled genomes of all isolates used in the study are available in FigShare DOI: 10.6084/m9.figshare.7886810.

C. coli and _C. jejuni_ phylogenies and assessing temporal signal and 'clock-likeness'

Phylogenies were constructed for 601 *C. coli* and 1,824 *C. jejuni* isolates (**S1 Table, Fig 1**). Gene-by-gene alignments were produced with comparison to reference *C. coli* (YH501, accession number NZ_CP015528.1) and *C. jejuni* (NCTC11168, accession number NC_002163.1) isolate genomes, sampled in 2016 and 1977 respectively. These reference genomes, belonging to the ST-828 and ST-21 clonal complexes, were chosen as those most commonly used in *Campylobacter* comparative population genomics studies [77,78]. Homology to the reference was determined using MAFFT, with default parameters of minimum nucleotide identity of 70% over >50% of the gene and a BLAST-n word size of 20. Core genes (2,014 for *C. coli* and 1,668 for *C. jejuni*), shared by all isolates within a species were concatenated and used to construct Maximum likelihood (ML) trees using FastTree version 2.1.8 and the Generalised time-reversible (*GTR*) model of nucleotide evolution [79]. Isolates were analysed to test for a temporal signal of the accumulation of genetic variation over time (**S1 and S2 Figs**). This was carried out prior to NC rate analysis using a phylogeny of genetic distances and sampling dates, and root-to-tip regression implemented in the software TempEst v1.5.1 [80] with the best fitting root selected to maximise the coefficient, R^2. Core genome phylogenies contained dated-tip isolates sampled between 1970 and 2016 for *C. coli* and *C. jejuni*.

Root-to-tip regression analyses to identify a temporal signal in bacteria rely on the removal of recombination as this is often the main source of genetic variation. Such analyses have been performed on small genome collections (15-189 isolates) of multiple bacterial species [44]. However, for *Campylobacter*, this would not be sufficient to represent diversity within the species as there are >40 known clonal complexes within *C. jejuni* alone. Using existing methodology, it was not possible to exclude recombining regions and perform root-to-tip

regression on the entire *C. jejuni* (1824 isolates) and *C. coli* (601 isolates) genome collections. Therefore, we conducted analyses on sub-lineages within *C. jejuni* and *C. coli*.

In order to identify temporal signal using TempEst, individual subsets of *Campylobacter* lineages were chosen from our datasets for *C. coli* (ST-825, ST-827, ST-828, ST-830, ST-872, ST-1090 and ST-1541 of the clonal complex, ST-828) and *C. jejuni* (ST-1325, ST-1034, ST-206, ST-21, ST-22, ST-257, ST-353, ST-354, ST-42, ST-433, ST-45, ST-464, ST-48, ST-52, ST-574, ST-61, ST-658 and ST-661 clonal complexes). Core genes were identified for each sub-lineage by comparison to *C. coli* (YH501) and *C. jejuni (*NCTC 11168) reference genomes using MAFFT (as described above). Individual ML phylogenies were constructed from core gene alignments using FastTree. Recombined regions were inferred using ClonalFrameML with basic model parameters [81] and removed using a cfml-mask script and replaced with gaps (https://github.com/kwongj/cfml-maskrc). Recombination-masked trees of individual lineages were subsequently tested for temporal signal using TempEst software v1.5.1.

Bayesian evolutionary analysis

Analysis with BEAST2 v2.5.0 [45] was performed using a method previously described for *Campylobacter* [8]. SNP alignments were constructed from variable sites of the whole datasets of 601 (*C. coli*) and 1824 (*C. jejuni*) isolates and for the sub-lineages which exhibited the strongest temporal signal using snp-sites v2.5.1 [82]. A time-scale phylogeny was constructed using BEAST2 v2.5.0 [45] based on variable sites, using the GTR +G4 model of DNA substitution. The relaxed log-normal clock with Bayesian skyline model was used as previously described [8]. Input xml files were prepared using BEAUti2 v2.5.0 [45]. A prior on the clock rate was set as a log-normal distribution with a mean value of 1 x 10^{-6} mutations per site per

year with a lower value of 1 x 10^{-8} and an upper value of 1 x 10^{-3}. Markov chains were run for 50 million generations, sampled every 10,000 generations with the first 5,000,000 generations (10%) discarded as burn-in.

Selection of closely related isolate pairs

An ideal dataset for rate analysis would include isolate pairs with divergent sampling dates, sufficient to measure NC rates over time, while remaining close enough (clustering on the tree) to share reliable recent common ancestry. Furthermore we required as many pairs as possible for confidence in average rates. In order to achieve this, pairwise nucleotide identity and year between isolation date matrices were constructed separately for 601 (*C. coli*) and 1,824 (*C. jejuni*) isolates. Using a bespoke R script (https://github.com/SionBayliss/CallandMolClock), the distribution of nucleotide identity was determined for isolate pairs within sequential isolation date categories of 1 year or more (1-37 for *C. coli*, 1-46 for *C. jejuni*) by comparing every isolate to all other isolates (**Fig 2**). In each analysis, isolates were used only once as the ancestral or derived strain.

Recombination and nucleotide change inference

The raw reads of genomes (**S1 Table**) of isolate pairs (**Table 1**) were mapped to the complete reference genomes: *C. coli* YH501 (accession: NZ_CP015528.1) and *C. jejuni* NCTC 11168 (accession: NC_002163.1) using the BWA-MEM algorithm [83]. Variants were called using Freebayes v1.1.0-dirty [84] and NC effects predicted and annotated using SnpEff version 4.3 [85] (**S5 Table**). These tools were included in the haploid variant calling pipeline, 'snippy' v3.0 (https://github.com/tseemann/snippy). Core genome sub-tree alignments were constructed using snippy-core. NCs introduced by point mutation and recombination were inferred on the

alignments using Gubbins v2.4.1 (default settings) [86] for each isolate pair (**S5 Table**). The snippy pipeline was used to identify synonymous and non-synonymous NCs within and outside of inferred recombinant regions [86]. *dN/dS* ratios were calculated for sites across the core genome using the synonymous/non-synonymous analysis program (SNAP) v2.1.1 based on the Nei and Gojobori 1986 method [87,88] (www.hiv.lanl.gov). Rates were calculated by reconstructing the NCs on internal branches (inferred using Gubbins) leading to the MRCA shared by a pair of isolates. By quantifying point mutation and recombination and synonymous and nonsynonymous NCs per branch, we were able to infer different molecular evolution rate estimates based on the difference in isolation time between isolates pairs (**S3 Fig C**)**.** These included (i) the total NC rate, used to calculate the number of effective lineages and (ii) the rate of accumulation of synonymous NCs occurring outside of recombinant regions, used to estimate the molecular clock. Hotspots of recombination occurring across multiple isolate pairs were observed.

Estimating the number of coalescences at yearly intervals (Birthday problem)

To consider the extent to which a given sample set represented genetic diversity within the population we developed a pipeline that calculated the number of coalescences (*effective lineages,* **Z**) at yearly time intervals (Z1, Z2, Z3….Zn) within the datasets. This is described by the equation **Z** = **Y/X,** Where: **Y** = all potential isolate pairs ($n^2/2$); **X** = the number of possible pairs for each time interval (*t1, t2,t3….tn*) that is less than the predicted number of NCs that have occurred over a given time interval ($\mu(t(1-n))$; $\boldsymbol{\mu}$ = rate of nucleotide change; $\boldsymbol{t}$ = time interval between sampling dates, 1-46 and 1-37 years for *C. jejuni* and *C. coli* respectively. The resultant **Z** value for each time period is the estimated number of effective lineages (Birthdays)

at each time cut-off, equivalent to the number of lineages sharing a common ancestor at a particular time interval (**S3 Fig**).

Acknowledgements

JKC, SKS and DF designed the study and wrote the paper with BP. JKC, BP performed genomic analysis with input from HT, SCB and EJF. EB and MB cultured isolates for sequencing. EM, MDH and BP sequenced and assembled genomes. All authors contributed and approved the final manuscript.

References

1. Kimura M. Evolutionary rate at the molecular level. Nature 1968;217(5129):624-626.
2. Kuo CH, Ochman H. Inferring clocks when lacking rocks: the variable rates of molecular evolution in bacteria. Biol Direct. 2009;4:35.
3. Didelot X, Walker AS, Peto TE, Crook DW, Wilson DJ. Within-host evolution of bacterial pathogens. Nat Rev Microbiol. 2016;14:150-162.
4. Kidgell C, Reichard U, Wain J, Linz B, Torpdahl M, Dougan G, Achtman M. Salmonella typhi, the causative agent of typhoid fever, is approximately 50,000 years old. Infect Genet Evol. 2002;2(1):39–45.
5. Mutreja A, Kim DW, Thomson NR, Connor TR, Lee JH, Kariuki S, Croucher NJ, Choi SY, Harris SR, Lebens M, et al. Evidence for several waves of global transmission in the seventh cholera pandemic. Nature 2011;477(7365):462–465.

6. Mcadam PR, Templeton KE, Edwards GF, Holden MTG, Feil EJ, Aanensen DM, Bargawi HJA, Spratt BG, Bentley SD, Parkhill J, et al. Molecular tracing of the emergence, adaptation, and transmission of hospital-associated methicillin-resistant Staphylococcus aureus. Proc Natl Acad Sci U S A. 2012;109(23):9107–9112.
7. Cui Y, Yu C, Yan Y, Li D, Li Y, Jombart T, Weinert LA, Wang Z, Guo Z, Xu L, et al. Historical variations in mutation rate in an epidemic pathogen, Yersinia pestis. Proc Natl Acad Sci U S A. 2013;110(2):577–582.
8. Mourkas E, Taylor AJ, Meric G, Bayliss SC, Pascoe B, Mageiros L, Calland JK, Hitchings MD, Ridley A, Vidal A, et al. Agricultural intensification and the evolution of host specialism in the enteric pathogen Campylobacter jejuni. PNAS 2020;117(20):11018-11028.
9. Weller C, Wu M. A generation-time effect on the rate of molecular evolution in bacteria. Evolution (N Y). 2015;69(3):643–652.
10. Gibson B, Wilson D, Feil E, Eyre-Walker A. The Distribution of Bacterial Doubling Times in the Wild. Proc Biol Sci. 2018;285(1880).
11. Vos M, Didelot X. A comparison of homologous recombination rates in bacteria and archaea. ISME J. 2009;3(2):199–208.
12. Bromham L. Why do species vary in their rate of molecular evolution? Biol Lett. 2009;5:401-404.
13. Eyre-Walker A, Keightley PD. The distribution of fitness effects of new mutations. Nat Rev Gen. 2007;8:610-618.
14. Gibson B, Eyre-Walker A. Investigating evolutionary rate variation in bacteria. J Mol Evol. 2019;87:317-326.

15. Drummond AJ, Pybus OG, Rambaut A, Forsberg R, Rodrigo AG. Measurably evolving populations. Trends Ecol Evol. 2003;18:481–488.
16. Biek R, Pybus OG, Lloyd-Smith JO, Didelot X. Measurably evolving pathogens in the genomic era. Trends Ecol Evol. 2015;30(6):306–313.
17. Drummond AJ, Rambaut A. BEAST: Bayesian evolutionary analysis by sampling trees. BioMed Cent. 2007;7(214):1–8.
18. Suchard MA, Lemey P, Baele G, Ayres DL, Drummond AJ, Rambaut A. Bayesian phylogenetic and phylodynamic data integration using BEAST 1.10. Virus Evol 2018;8:4(1):vey016.
19. Arnold BJ, Hanage WP. Longitudinal samples of bacterial genomes potentially bias evolutionary analyses. Unpublished data bioRxiv 2017 https://www.biorxiv.org/content/10.1101/103465v1, last accessed October 18, 2020
20. Maixner F, Krause-Kyora B, Turaev D, Herbig A, Hoopmann MR, Hallows JL, Kusebauch U, Egarter Vigl E, Malfertheiner P, Megraud F, et al. The 5,300-year-old Helicobacter pylori genome of the Iceman HHS Public Access. Science 2016;351(6269):162–165.
21. Didelot X, Eyre DW, Cule M, Ip CLC, Ansari MA, Griffiths D, Vaughan A, O'Connor L, Golubchik T, Batty EM, et al. Microevolutionary analysis of Clostridium difficile genomes to investigate transmission. Genome Biol. 2012;13(12):R118.
22. Walker TM, C Ip CL, Harrell RH, Evans JT, Kapatai G, Dedicoat MJ, Eyre DW, Wilson DJ, Hawkey PM, Crook DW, et al. Whole-genome sequencing to delineate Mycobacterium tuberculosis outbreaks: a retrospective observational study. Lancet Infect Dis. 2013;13:137–146.

23. Mathers AJ, Stoesser N, Sheppard AE, Pankhurst L, Giess A, Yeh AJ, Didelot X, Turner SD, Sebra R, Kasarskis A, et al. Klebsiella pneumoniae Carbapenemase (KPC)-Producing K. pneumoniae at a Single Institution: Insights into Endemicity from Whole-Genome Sequencing. Antimicrob Agents Chemother. 2015;59:1656–1663.
24. Menardo F, Duchêne S, Brites D, Gagneux S. The molecular clock of Mycobacterium tuberculosis. PLoS Pathog. 2019;15(9):e1008067.
25. Waldenström J, Broman T, Carlsson I, Hasselquist D, Achterberg RP, Wagenaar JA, Olsen B. Prevalence of Campylobacter jejuni, Campylobacter lari, and Campylobacter coli in different ecological guilds and taxa of migrating birds. Appl Environ Microbiol. 2002;68(12):5911–5917.
26. Sheppard SK, Colles FM, Mccarthy ND, Strachan NJC, Ogden ID, Forbes KJ, Dallas JF, Maiden MCJ. Niche segregation and genetic structure of Campylobacter jejuni populations from wild and agricultural host species. Mol Ecol. 2011;20(16):3484–3490.
27. Bronowski C, James CE, Winstanley C. Role of environmental survival in transmission of *Campylobacter jejuni*. FEMS Microbiol Lett. 2014;356(1):8–19.
28. Cody AJ, McCarthy ND, Bray JE, Wimalarathna HML, Colles FM, Jansen van Rensburg MJ, Dingle KE, Waldenstrom J, Maiden MCJ. Wild bird-associated Campylobacter jejuni isolates are a consistent source of human disease, in Oxfordshire, United Kingdom. Env Micro Reports. 2015;7(5)782-788.
29. Sheppard SK, Maiden MCJ. The evolution of Campylobacter jejuni and Campylobacter coli. Cold Spring Harb Perspec Biol. 2015;7(8):a018119.
30. Wilson DJ, Gabriel E, Leatherbarrow AJH, Cheesbrough J, Gee S, Bolton E, Fox A, Fearnhead P, Hart CA, Diggle PJ. Tracing the Source of Campylobacteriosis. PLoS Genet. 2008;4(9):e1000203.

31. Sheppard SK, Dallas JF, Strachan NJC, MacRae M, McCarthy ND, Wilson DJ, Gormley FJ, Falush D, Ogden ID, Maiden MCJ, et al. Campylobacter genotyping to determine the source of human infection. Clin Infect Dis. 2009;48(8):1072–1078.
32. Strachan NJC, Gormley FJ, Rotariu O, Ogden ID, Miller G, Dunn GM, Sheppard SK, Dallas JF, Reid TMS, Howie H, et al. Attribution of *Campylobacter* Infections in Northeast Scotland to Specific Sources by Use of Multilocus Sequence Typing. J Infect Dis. 2009;199(8):1205–1208.
33. Dearlove BL, Cody AJ, Pascoe B, Méric G, Wilson DJ, Sheppard SK. Rapid host switching in generalist Campylobacter strains erodes the signal for tracing human infections. 2016;ISME J. 10(3):721–729.
34. Rosner BM, Schielke A, Didelot X, Kops F, Breidenbach J, Willrich N, Gölz G, Alter T, Stingl K, Josenhans C, et al. A combined case-control and molecular source attribution study of human Campylobacter infections in Germany, 2011–2014. Sci Rep. 2017;7(1):5139.
35. Thépault A, Méric G, Rivoal K, Pascoe B, Mageiros L, Touzain F, Rose V, Béven V, Chemaly M, Sheppard SK. Genome-Wide Identification of Host- Segregating Epidemiological Markers for Source Attribution in Campylobacter jejuni. Appl Environ Microbiol. 2017;83(7).
36. Marin J, Hedges SB. Undersampling genomes has biased time and rate estimates throughout the tree of life. Mol Biol Evol. 2018;35(10):2595.
37. Mathis, FH. A generalized birthday problem. SIAM review. 1991;33(2):265-270.
38. Jolley KA, Bray JE, Maiden MCJ. Open-access bacterial population genomics: BIGSdb software, the PubMLST.org website and their applications. Wellcome Open Res. 2018;24(3):124.

39. Didelot X, Falush D. Inference of Bacterial Microevolution Using Multilocus Sequence Data. Genetics. 2007;175(3):1251–1266.
40. Kimura M. Molecular evolutionary clock and the neutral theory. J Mol Evol. 1987;26(1–2):24–33.
41. Gojobori T, Moriyama EN, Kimura M. Molecular clock of viral evolution, and the neutral theory. Proc Natl Acad Sci U S A. 1990;87(24):10015-10018.
42. Rieux A, Balloux F. Inferences from tip-calibrated phylogenies: a review and a practical guide. Mol Ecol. 2016;25(9):1911–1924.
43. Sheppard SK, Cheng L, Méric G, De Haan CPA, Llarena AK, Marttinen P, Vidal A, Ridley A, Clifton-Hadley F, Connor TR, et al. Cryptic ecology among host generalist Campylobacter jejuni in domestic animals. Mol Ecol. 2014;23(10):2442–2451.
44. Duchêne S, Holt KE, Weill F-X, Le Hello S, Hawkey J, Edwards DJ, Fourment M, Holmes EC. Genome-scale rates of evolutionary change in bacteria. Microb Genomic. 2016;2(11).
45. Bouckaert R, Vaughan TG, Barido-Sottani J, Duchene S, Fourment M, Gavryushkina A, Heled J, Jones G, Kuhnert D, De Maio N, et al. BEAST 2.5: An advanced software platform for Bayesian evolutionary analysis. PLoS Comput Biol. 2019;15(4):e1006650.
46. Ho SYW, Phillips MJ, Cooper A, Drummond AJ. Time dependency of molecular rate estimates and systematic overestimation of recent divergence times. Mol Biol Evol. 2005;22(7):1561-1568.
47. Wilson DJ, Gabriel E, Leatherbarrow AJH, Cheesbrough J, Gee S, Bolton E, Fox A, Hart CA, Diggle PJ, Fearnhead P. Rapid evolution and the importance of recombination to the gastroenteric pathogen Campylobacter jejuni. Mol Biol Evol. 2009;26(2):385–397.

48. Rocha EPC, Smith JM, Hurst LD, Holden MTG, Cooper JE, Smith NH, Feil EJ. Comparisons of dN/dS are time dependent for closely related bacterial genomes. J Theor Biol. 2006;239:226–235.
49. Castillo-Ramirez S, Harris SR, Holden MTG, He M, Parkhill J, Bentley SD, Feil EJ. The impact of recombination on dN/dS within recently emerged bacterial clones. PLoS Pathog. 2011;(7):e1002129.
50. Kryazhimskiy S, Plotkin JB. The population genetics of dN/dS. PLoS genet. 2008;4(12), e1000304.
51. Yahara K, Didelot X, Ansari MA, Sheppard SK, Falush D. Efficient inference of recombination hot regions in bacterial genomes. Molecular Biology and Evolution 2014;31(6): 1593-1605.
52. Croucher NJ, Harris SR, Fraser C, Quail MA, Burton J, Van Der Linden M, Mcgee L, Von Gottberg A, Song JH, Ko KS, et al. Rapid Pneumococcal Evolution in Response to Clinical Interventions. Science 2011;331(6016):430–434.
53. von Mering C, Hugenholtz P, Raes J, Tringe SG, Doerks T, Jensen LJ, Ward N, Bork P. Quantitative Phylogenetic Assessment of Microbial Communities in Diverse Environments. Science 2007;315(5815):1126–1130.
54. Li S-J, Hua Z-S, Huang L-N, Li J, Shi S-H, Chen L-X, Kuang J-L, Liu J, Hu M, Shu W-S. Microbial communities evolve faster in extreme environments. Sci Rep. 2015;4(1):6205.
55. Denamur E, Matic I. Evolution of mutation rates in bacteria. Mol Microbiol. 2006;60(4).
56. Ho SYW, Shapiro B, Phillips MJ, Cooper A, Drummond AJ, Sullivan J. Evidence for Time Dependency of Molecular Rate Estimates. Sullivan J, editor. Syst Biol. 2007;56(3):515–522.

57. Ho SYW, Lanfear R, Bromham L, Phillips MJ, Soubrier J, Rodrigo AG, Cooper A. Time-dependent rates of molecular evolution. Mol Ecol. 2011;20(15):3087–3101.

58. Duchêne S, Holmes EC, Ho SYW. Analyses of evolutionary dynamics in viruses are hindered by a time-dependent bias in rate estimates. Proceedings Biol Sci. 2014;281(1786).

59. Kirchberger PC, Schmidt ML, Ochman H. The ingenuity of bacterial genomes. Annu Rev Microbiol. 2020;8;74:815-834.

60. Cui Y, Yang X, Didelot X, Guo C, Li D, Yan Y, Zhang Y, Yuan Y, Yang H, Wang J et al. Epidemic clones, oceanic gene pools, and eco-LD in the free-living marine pathogen Vibrio parahaemolyticus. Mol Biol Evol. 2015;32(6):1396-410.

61. Louca S, Shih PM, Pennell MW, Fischer WW, Parfrey LW, Doebeli M. Bacterial diversification through geological time. Nat Ecol Evol. 2018;2, 1458-1467.

62. Koeppel A, Perry EB, Sikorski J, Krizanc D, Warner A, Ward DM, Rooney AP, Brambilla E, Connor N, Ratcliff RM, et al. Identifying the fundamental units of bacterial diversity: A paradigm shift to incorporate ecology into bacterial systematics. PNAS 2008;105(7):2504-2509.

63. den Bakker HC, Didelot X, Fortes ED, Nightingale KK, Wiedman M. Lineage specific recombination rates and microevolution in Listeria monocytogenes. BMC Evol Biol. 2008;8;277. doi: 10.1186/1471-2148-8-277.

64. Sheppard SK, Dallas JF, Wilson DJ, Strachan NJC, McCarthy ND, Jolley KA, Colles FM, Rotariu O, Ogden ID, Forbes KJ, et al. Evolution of an Agriculture-Associated Disease Causing Campylobacter coli Clade: Evidence from National Surveillance Data in Scotland. Hartskeerl RA, editor. PLoS One. 2010;5(12):e15708.

65. Sheppard SK, McCarthy ND, Falush D, Maiden MCJ. Convergence of Campylobacter species: implications for bacterial evolution. Science 2008;320(5873):237-239.
66. Sheppard SK, Didelot X, Jolley KA, Darling AE, Pascoe B, Meric G, Kelly DJ, Cody A, Colles FM, Strachan NJC, et al. Progressive genome-wide introgression in agricultural Campylobacter coli. Mol Ecol. 2013;22(4)1051-1064.
67. Rainey PB, Travisano M. Adaptive radiation in a heterogeneous environment. Nature. 1998;394(6688):69-72.
68. Flohr RCE, Blom CJ, Rainey PB, Beaumont HJE. Founder niche constrains evolutionary adaptive radiation. PNAS. 2013;110(51):20663-20668.
69. Thakur S, Morrow WEM, Funk JA, Bahnson PB, Gebreyes WA. Molecular epidemiologic investigation of Campylobacter coli in swine production systems, using multilocus sequence typing. Appl Environ Microbiol. 2006;72(8):5666-5669.
70. Croucher NJ, Finkelstein JA, Pelton SI, Mitchell PK, Lee GM, Parkhill J, Bentley SD, Hanage WP, Lipsitch M. Population genomics of post-vaccine changes in pneumococcal epidemiology. Nat Genet. 2013;45:656–663.
71. Didelot X, Nell S, Yang I, Woltemate S, Van Der Merwe S, Suerbaum S. Genomic evolution and transmission of Helicobacter pylori in two South African families. Proc Natl Acad Sci U S A. 2013;110(34):13880–13885.
72. Everitt RG, Didelot X, Batty EM, Miller RR, Knox K, Young BC, Bowden R, Auton A, Votintseva A, Larner-Svensson H, et al. Mobile elements drive recombination hotspots in the core genome of Staphylococcus aureus. Nat Commun. 2014;5(3956).
73. Bar-On YM, Phillips R, Milo R. The biomass distribution on Earth. Proc Natl Acad Sci. 2018;115(25):6506–6511.

74. Dhillon AS, Shivaprasad HL, Schaberg D, Wier F. Campylobacter jejuni in broiler chickens. Avian Diseases. 2006;50(1):55-58.
75. Bankevich A, Nurk S, Antipov D, Gurevich AA, Dvorkin M, Kulikov AS, Lesin VM, Nikolenko SI, Pham S, Prjibelski AD, et al. SPAdes: A new genome assembly algorithm and its applications to single-cell sequencing. J Comput Biol. 2012;19(5):455-477.
76. Jolley KA, Maiden MC. BIGSdb: Scalable analysis of bacterial genome variation at the population level. BMC Bioinformatics. 2010;11:595.
77. Ghatak S, He Y, Reed S, Strobaugh Jr T, Irwin P. Whole genome sequencing and analysis of Campylobacter coli YH502 from retail chicken reveals a plasmid-borne type VI secretion system. Genom Data. 2017;11:128-131.
78. Pascoe B, Williams LK, Calland JK, Meric G, Hitchings MD, Dyer M, Ryder J, Shaw S, Lopes BS, Chintoan-Uta C, et al. Domestication of Campylobacter jejuni NCTC 11168. Microb Genom. 2019;5(7):e000279.
79. Price MN, Dehal PS, Arkin AP. FastTree 2 – Approximately Maximum-Likelihood Trees for Large Alignments. Poon AFY, editor. PLoS One. 2010;5(3):e9490.
80. Rambaut A, Lam TT, Carvalho LM, Pybus OG. Exploring the temporal structure of heterochronous sequences using TempEst (formerly Path-O-Gen). Virus Evol. 2016;2(1).
81. Didelot X, Wilson DJ. ClonalFrameML: Efficient inference of recombination in whole bacterial genomes. PLoS Comput Biol. 2015;11(2): e1004041.
82. Page AJ, Taylor B, Delaney AJ, Soares J, Seeman T, Keane JA, Harris SR. SNP-sites: rapid efficient extraction of SNPs from multi-FASTA alignments. Microb Genom. 2016;2(4):e000056.

83. Li H. Aligning sequence reads, clone sequences and assembly contigs with BWA-MEM. 2013;Unpublished data, arXiv:1303.3997v2 [q-bio.GN]. Last accessed on October 18 2020
84. Garrison E, Marth G. Haplotype-based variant detection from short-read sequencing. 2012;Unpublished data, arXiv preprint arXiv:1207.3907 [q-bio.GN]. Last accessed on November 24 2020.
85. Cingolani P, Platts A, Wang LL, Coon M, Nguyen T, Luan Wang SJL, Ruden DM. A program for annotating and predicting the effects of single nucleotide polymorphisms, SnpEff: SNPs in the genome of Drosophila melanogaster strain w1118; iso-2; iso-3. Fly. 2012;6(2):80–92.
86. Croucher NJ, Page AJ, Connor TR, Delaney AJ, Keane JA, Bentley SD, Parkhill J, Harris SR. Rapid phylogenetic analysis of large samples of recombinant bacterial whole genome sequences using Gubbins. Nucleic Acids Res. 2015;43(3):e15.
87. Nei M, Gojobori T. Simple methods for estimating the numbers of synonymous and nonsynonymous nucleotide substitutions. Mol Biol Evol. 1986;3(5):418-426.
88. Korber B. HIV Signature and Sequence Variation Anaylsis. Computational Analysis of HIV Molecular Sequences, Allen G. Rodrigo and Gerald H. Learn, eds. Dordrecht, Netherlands: Kluwer Academic Publishers, 2000. Chapter 4, pages 55-72.

Supporting Information

S1 Table. Isolate list information

S2 Table. TempEst root-tip regression and BEAST analysis estimates (*C. coli*)

S3 Table. TempEst root-to-tip regression and BEAST analysis estimates (*C. jejuni*)

S4 Table. List of possible pairs of isolates

S5 Table. Additional NC annotations

S6 Table. Individual pair rates

Fig 1. Little evidence of clustering of isolate sampling dates in *Campylobacter* phylogenies. Maximum likelihood (ML) core genome phylogenetic trees of *C. coli* (A) (n = 601) and *C. jejuni* (B) (n = 1824) constructed using FastTree version 2.1.8 [79] and the *GTR* model of nucleotide evolution. Both phylogenies show the distribution of the sample time frame used in this study with major *Campylobacter* clonal complexes (CCs) identified and terminal nodes coloured according to isolation decade (orange = 1970s, yellow = 1980s, white = 1990s, green = 2000s, blue = 2010s). Scale bars represent the estimated number of NCs per site. Terminal nodes sampled from different decades can be seen scattered throughout both trees with little evidence of clustering by decade. Isolates sampled from the 2000s and 2010s are most abundant within each dataset. The position of the *C. jejuni* (NCTC11168) and *C. coli* (YH501) reference genomes are indicated on the phylogeny. These were sampled in 1977 and 2016 respectively.

Fig 2. Pair selection criteria curves for inclusion in rate estimates. Visual representation of possible pairs of isolates at all time cut-offs across the sample time frame for *C. jejuni* (B) and *C. coli* (D). As time difference between pairs increases, distinguishing between individual curves becomes distorted. Therefore, a selection of years were plotted (A and C) (black = all pairs >1 year difference, blue = >2 years, pink = >4 years, purple = >6 years, orange = >8 years, red = >10 years, green = >15 years). All isolates were paired with the nearest isolate (genetic distance), matched according to difference in year of isolation (coloured lines) for both *C. jejuni* (A) and *C. coli* (C) (orange line). Dashed boxes (A and C) show magnified images of the closest pairs from all curves. The 20 and 18 pairs used in rate calibration are highlighted by a black

oval (A) and every orange pair in dashed box (C). Grey scale bars (B and D) indicate the time difference cut-off of each curve for every time point in the sample date frame.

Fig 3. Mutation and recombination in *C. coli* and *C. jejuni*. Average genome-wide NC positions (red dots = synonymous NCs, blue dots = nonsynonymous NCs) per isolate pair in relation to inferred recombined regions (grey blocks). Each plot represents one pair of isolates considered in rate calibration for *C. coli* (A) and *C. jejuni* (B) and are ordered according to Table 1. *y axis* = number of NCs in relation to particular bp position of the reference genome (*C. coli* = YH501, *C. jejuni* = NCTC11168) and varies between pairs. *x axis* = position of reference genome in bins of 10,000 bp. The cladogram shows the relatedness of isolate pairs based on nucleotide identity, scale bar indicates NCs per site. It is evident from both A and B that recombination is the main source of variation in *C. coli* and *C. jejuni*.

Fig 4. Lineage expansion in *C. jejuni* and *C. coli*. (A) Number of effective lineages (y axis) at each time point within the sample time frame (x axis) for *C. coli* (grey) and *C. jejuni* (black). (B) Diagrammatic representation of lineage expansion in *C. coli* and *C. jejuni* showing contrasting lineage diversification scenarios.

S1 Fig. Root-to-tip linear regression of *C. coli* implemented in the software, TempEst. Root-to-tip genetic distance (y axis) is correlated with sampling time (x axis) for phylogenies of (A) 601 *C. coli* and (B) 8 sub-lineages of the ST-828 clonal complex. Only 3 out of 8 sub-lineages had strong temporal signal ($R^2 > 0.5$).

S2 Fig. Root-to-tip linear regression of *C. jejuni* implemented in the software, TempEst. Root-to-tip genetic distance (y axis) is correlated with sampling time (x axis) for phylogenies of (A) 1824 *C. jejuni* and (B) 18 sub-lineages representing *C. jejuni* clonal complexes. Only 5 out of 18 sub-lineages had strong temporal signal ($R^2 > 0.5$).

S3 Fig. Methods for calculating the number of effective lineages within the population. (A) The total number of *C. jejuni* and *C. coli* isolates in the population and all potential pairwise comparisons between putative ancestral (black) and contemporary (white) strains to give the total number of potential isolate pairs, Y. (B) Isolate pair selection based on divergent sampling date (>8 years) and a nucleotide identity threshold <5000 SNPs. (C) Total rate of nucleotide change (μ) calculated for all chosen pairs. The rate of accumulation of all synonymous (S), nonsynonymous (N) NCs, within (rec) and outside (mut) of recombined regions, was estimated since the most recent common ancestor (MRCA, red circle). The difference in NCs between each pair was divided by the difference in isolation years to give μ. (D) The total NC rate was used to estimate the number of NCs that were to accumulate over a time period and the number of possible isolate pairs at given time intervals (t*1, t2,t3….tn*) for each species.

Table 1: Isolate pair information for *Campylobacter coli*

Pair no.	Isolate	Year of isolation	ST*	CC**	Source	Country	Difference in years
1	4316.LDI12946	2006	827	ST-828CC	Environmental	UK	8
	3158.LDI6744	2014	827	ST-828CC	Environmental	UK	
2	4281.LDI12911	2007	827	ST-828CC	Environmental	UK	8
	3804.CCN182coli	2015	827	ST-828CC	Duck	UK	
3	1783.SS_328	2006	827	ST-828CC	Cattle	UK	8
	3166.LDI6752	2014	827	ST-828CC	Environmental	UK	
4	454.SS_047	2005	827	ST-828CC	Chicken	UK	8
	3150.LDI6736	2013	827	ST-828CC	Environmental	UK	
5	3899.H042120298	2004	962	ST-828CC	Environmental	UK	8
	2701.OXC6817	2012	962	ST-828CC	Human	UK	
6	1770.SS_018	2006	827	ST-828CC	Chicken	UK	8
	3160.LDI6746	2014	827	ST-828CC	Environmental	UK	
7	439.SS_031	2005	827	ST-828CC	Chicken	UK	8
	3152.LDI6738	2013	827	ST-828CC	Environmental	UK	
8	1789.SS_335	2006	827	ST-828CC	Wild bird	UK	8
	3174.LDI6760	2014	827	ST-828CC	Environmental	UK	
9	1798.SS_344	2001	827	ST-828CC	Chicken	UK	10
	1753.SS_273	2011	827	ST-828CC	Human	UK	
10	3766.H065100499	2006	827	ST-828CC	Environmental	UK	8
	3176.LDI6762	2014	827	ST-828CC	Environmental	UK	
11	3922.H054900335	2005	825	ST-828CC	Environmental	UK	8
	3161.LDI6747	2013	825	ST-828CC	Environmental	UK	
12	4348.LDI12978	2005	827	ST-828CC	Environmental	UK	8
	3154.LDI6740	2013	827	ST-828CC	Environmental	UK	
13	3925.H043900429	2004	827	ST-828CC	Environmental	UK	8
	2690.OXC6785	2012	827	ST-828CC	Human	UK	
14	3877.H054000445	2005	825	ST-828CC	Environmental	UK	8
	3169.LDI6755	2013	825	ST-828CC	Environmental	UK	
15	1797.SS_343	2005	825	ST-828CC	Chicken	UK	8
	3162.LDI6748	2013	825	ST-828CC	Environmental	UK	
16	3800.UNOR5482c	2003	2195	ST-828CC	Environmental	UK	9
	1855.SS_614	2012	2195	ST-828CC	Human	UK	
17	3803.UNOR13691b	2003	827	ST-828CC	Environmental	UK	8
	1792.SS_338	2011	827	ST-828CC	Chicken	UK	
18	3167.LDI6753	2001	1541	ST-828CC	Environmental	UK	11
	1852.SS_595	2012	6795	ST-828CC	Human	UK	

Table 2: Isolate pair information for *Campylobacter jejuni*

Pair no.	Isolate	Year of isolation	ST*	CC**	Source	Country	Difference in years
1	5932.Manchester	2003	43	ST-21CC	Human	UK	13
	29.NC_002163	2016	43	ST-21CC	Human	UK	
2	275.13264	1999	257	ST-257CC	Human	UK	12
	2140.OXC5779	2011	257	ST-257CC	Human	UK	
3	267.13256	1991	42	ST-42CC	Human	UK	12
	85.cow3583	2003	3583	ST-42CC	Cattle	UK	
4	5921.Aberdeen	2002	43	ST-21CC	Human	UK	14
	5855.LITTER.B.E	2016	43	ST-21CC	Chicken	UK	
5	269.13258	1998	48	ST-48CC	Lamb	UK	9
	1806.SS_381	2007	48	ST-48CC	Chicken	UK	
6	1776.SS_029	2005	45	ST-45CC	Chicken	UK	10
	4809.CTA244	2015	45	ST-45CC	Dog	France	
7	5735.79.23	1979	1457	ST-443CC	Duck	USA	32
	2397.Seal73	2011	1457	ST-443CC	Seal	UK	
8	255.Hn30	2003	50	ST-21CC	Human	UK	12
	4801.CTA093	2015	50	ST-21CC	Dog	France	
9	299.SS_202	2008	257	ST-257CC	Chicken	UK	8
	5814.A4.G	2016	257	ST-257CC	Chicken	UK	
10	303.SS_214	2008	48	ST-48CC	Chicken	UK	8
	5986.LE.72	2016	48	ST-48CC	Chicken	UK	
11	268.13257	1999	45	ST-45CC	Human	UK	12
	2533.OXC6314	2011	45	ST-45CC	Human	UK	
12	5592.RM1285	1997	50	ST-21CC	Chicken	USA	16
	5560.MTVDSCj07	2013	50	ST-21CC	Chicken	USA	
13	2928.SS_0890	1999	1326	ST-45CC	Wild Bird	Sweden	12
	2451.Seal186	2011	1326	ST-45CC	Seal	UK	
14	5038.CjRM3147	2001	22	ST-22CC	Human	Mexico	15
	5902.Camp_108c	2016	22	ST-22CC	Chicken	UK	
15	1800.SS_375	2007	45	ST-45CC	Chicken	UK	8
	4811.CTA277	2015	45	ST-45CC	Dog	France	
16	463.SS_058	2005	45	ST-45CC	Chicken	UK	10
	5006.SS_2784	2015	1701	ST-45CC	Chicken	UK	
17	62.cowa21	2006	21	ST-21CC	Cattle	UK	9
	4834.CTA710	2015	21	ST-21CC	Dog	France	
18	5738.79.248	1979	50	ST-21CC	Turkey	USA	30
	5595.WP2202	2009	50	ST-21CC	Chicken	USA	
19	272.13261	1998	61	ST-61CC	Cattle	UK	18
	191.Cj2008.872	2016	61	ST-61CC	Human	France	
20	5743.79.315	1979	50	ST-21CC	Human	USA	36
	4832.CTA693	2015	50	ST-21CC	Dog	France	

Table 3: Estimates of evolutionary potential of nucleotide change across all *C. coli* genomes in each pair of isolates

	NCs in rec		NCs out rec						
Pair no.	**S**	**N**	**S**	**N**	**rdN/dS**	**mdN/dS**	**NCs/year***	**mol. clock rates****	**Total NC rate (m + r)/yr*****
1	202	249	61	105	0.731	0.541	-17.375	-6.000	-78.375
	0	0	13	20	0.000	0.575			
2	0	0	0	0	0.000	0.595	6.500	1.875	32.000
	104	95	15	34	0.473	0.597			
3	167	170	8	14	0.474	0.564	6.000	2.000	45.500
	276	349	24	31	0.362	0.558			
4	0	0	0	0	0.000	0.540	23.125	6.250	65.000
	171	157	50	113	0.540	0.619			
5	0	0	0	0	0.000	0.595	20.000	10.250	171.750
	609	569	82	64	0.564	0.509			
6	110	138	17	24	0.578	0.653	-2.125	-1.375	28.375
	199	284	6	17	0.376	0.571			
7	74	96	8	10	0.744	0.542	5.125	1.375	54.875
	350	210	19	35	0.692	0.579			
8	283	295	14	16	0.938	0.611	2.875	0.375	3.125
	247	314	17	23	0.288	0.543			
9	11717	6313	2467	1520	0.598	0.528	-256.400	-151.200	-1228.200
	4905	3639	955	644	1.144	1.115			
10	40	44	1	0	0.482	0.554	4.000	1.125	69.750
	282	316	10	24	0.679	0.611			
11	7	7	11	10	1.177	0.566	-1.875	-1.250	-3.625
	2	1	1	4	0.000	0.585			
12	0	0	0	0	0.000	0.620	10.250	4.125	62.250
	257	140	33	45	0.527	0.575			
13	49	75	36	74	0.889	0.622	10.875	5.250	177.250
	702	645	78	112	0.575	0.562			
14	419	262	19	44	0.689	0.750	10.000	3.125	107.125
	899	524	44	90	0.720	0.548			
15	947	622	79	39	0.458	0.613	-8.875	-8.125	-174.250
	191	107	14	37	0.354	0.500			
16	549	370	58	64	0.493	0.581	-15.333	-6.444	-126.111
	0	0	0	0	0.464	0.588			
17	681	510	60	129	0.611	0.618	-3.125	1.625	110.500
	1102	932	73	96	0.592	0.580			
18	0	0	0	0	0.000	0.592	27.273	13.818	545.909
	3304	2220	152	127	0.515	0.474			
SD	2101.48	1204.22	431.68	266.48	0.311	0.101	62.649	36.435	339.754
Mean	801	546	123	99	0.492	0.594	11.457	4.266	113.339

*synonymous and nonsynonymous NC outside of recombination; **synonymous NCs outside of recombination; ***all NCs within and without of recombination

S = observed synonymous NCs, N = observed nonsynonymous NCs, SD = standard deviation

Table 4: Estimates of evolutionary potential of nucleotide change across all *C. jejuni* genomes in each pair of isolates

	NCs in rec		NCs out rec						
Pair no.	**S**	**N**	**S**	**N**	**rdN/dS**	**mdN/dS**	**NCs/year***	**mol. clock rates****	**Total NC rate (m + r)/yr*****
1	0	0	0	3	0.000	0.000	0.000	0.000	0.077
	0	1	0	1	0.000	0.000			
2	30	50	23	40	0.488	0.505	0.167	0.083	-6.750
	0	0	24	47	0.000	0.580			
3	0	0	0	0	0.000	0.521	9.667	3.250	10.667
	4	3	39	67	0.342	0.517			
4	0	0	0	1	0.000	0.000	0.571	0.000	0.571
	0	0	0	8	0.000	0.000			
5	314	157	33	48	0.462	0.565	-8.000	-2.556	-57.444
	18	20	10	14	2.236	0.524			
6	136	205	90	174	0.730	0.545	58.300	26.800	32.100
	20	62	358	432	0.649	0.511			
7	0	0	0	0	0.000	0.524	7.219	3.000	10.844
	52	61	96	118	0.667	0.534			
8	16	47	32	32	1.131	0.544	27.583	10.917	39.583
	67	128	163	212	0.684	0.569			
9	107	63	20	36	0.000	0.563	-5.500	-1.875	-27.250
	1	2	5	6	1.225	0.503			
10	0	0	1	4	0.000	0.500	7.125	1.875	27.125
	97	62	16	40	0.459	0.534			
11	0	0	0	0	0.000	0.534	9.583	2.750	10.250
	0	7	33	77	0.786	0.542			
12	242	114	50	61	0.635	0.547	-6.313	-2.875	-28.000
	3	8	4	11	0.605	0.598			
13	259	138	27	42	0.311	0.560	-5.500	-2.083	-39.667
	0	0	2	8	0.000	0.538			
14	31	29	2	11	0.406	0.515	4.333	2.067	13.067
	128	61	33	40	0.639	0.571			
15	370	211	64	88	0.508	0.513	45.125	23.500	-20.000
	16	50	252	288	0.322	0.577			
16	172	69	79	101	0.399	0.531	-19.600	-7.500	-44.400
	0	0	4	9	0.000	0.500			
17	37	62	117	210	0.550	0.565	-39.222	-13.000	-51.000
	0	0	0	0	0.000	0.521			
18	10	26	0	0	1.265	0.578	2.300	0.367	10.267
	174	88	11	47	0.632	0.542			
19	177	128	22	44	0.840	0.511	-0.833	0.056	0.556
	202	119	23	33	0.441	0.520			
20	270	201	24	39	0.639	0.482	3.972	1.278	-0.167
	121	204	70	125	0.576	0.566			
SD	102.78	67.13	72.07	89.59	0.461	0.165	20.772	9.085	27.767
Mean	77	59	43	63	0.490	0.509	13.534	5.424	14.101

*synonymous and nonsynonymous NC outside of recombination; **synonymous NCs outside of recombination; ***all NCs within and without of recombination

S = observed synonymous NCs, N = observed nonsynonymous NCs, SD = standard deviation

Table 5: Average rate calibrations in *C. coli* and *C. jejuni*

	C. coli			*C. jejuni*			
Rates of nucleotide change	**Min**	**Mean**	**Max**	**Min**	**Mean**	**Max**	**Units****
Total*	1.7 x 10-6	6.3 x 10-5	3.0 x 10-4	4.8 x 10-8	8.8 x 10-6	2.3 x 10-5	s/s/y
S and N (exc. rec)	1.6 x 10-6	6.4 x 10-6	1.5 x 10-6	1.0 x 10-7	8.5 x 10-6	3.6 x 10-5	s/s/y
S (inc. rec)	4.9 x 10-6	3.1 x 10-4	1.8 x 10-3	2.1 x 10-7	1.9 x 10-6	7.6 x 10-6	s/s/y
S (exc. rec) (molecular clock)	2.1 x 10-7	2.4 x 10-6	7.7 x 10-6	3.8 x 10-8	3.4 x 10-6	1.7 x 10-5	s/s/y
N (inc. rec)	4.4 x 10-8	2.4 x 10-5	1.1 x 10-4	5.0 x 10-8	1.4 x 10-6	4.8 x 10-6	s/s/y
N (exc. rec)	4.8 x 10-7	3.2 x 10-6	7.8 x 10-6	3.1 x 10-7	4.8 x 10-6	1.6 x 10-5	s/s/y

*all NCs from including (inc) and excluding (exc) recombination (rec); **NCs per site per year (*C. jejuni* = 1.6 Mbp, *C. coli* = 1.8 Mbp)

S = synonymous NCs, N = nonsynonymous NCs

Table 6: Recombination information for each isolate in each *C. coli* pair considered for rate calibration

Pair no.	Rec blocks from root of subtree	Rec blocks from last common ancestor	r/m	Genome length (bp)	Bases in clonal frame (bp)	% of recombined genome
1	16	9	8.407	1,627,573	1,588,753	2.99
	7	0	0.978	1,609,340	1,606,957	0.15
2	0	0	0.000	1,666,864	1,666,864	0.00
	7	7	3.923	1,665,656	1,659,185	0.39
3	167	15	35.708	1,617,708	1,220,734	24.90
	162	10	38.985	1,603,282	1,201,817	25.84
4	6	0	10.145	1,616,057	1,593,221	1.41
	15	5	16.141	1,507,717	1,468,305	3.14
5	7	0	5.457	1,651,605	1,614,910	2.22
	52	45	20.475	1,659,211	1,595,168	7.09
6	162	7	46.548	1,621,038	1,225,532	24.71
	161	6	38.660	1,613,935	1,209,402	25.67
7	163	6	44.503	1,613,236	1,215,532	25.05
	171	14	54.284	1,618,186	1,220,026	24.94
8	180	28	39.419	1,621,543	1,223,908	24.84
	160	8	37.994	1,615,211	1,210,318	25.65
9	191	191	6.901	1,579,494	1,287,491	28.63
	172	172	37.839	1,616,244	1,203,711	25.92
10	192	5	143.956	1,616,455	1,209,888	25.48
	197	10	152.767	1,598,501	1,190,972	26.38
11	33	1	48.051	1,648,672	1,514,755	8.12
	32	0	47.809	1,649,085	1,515,390	8.11
12	2	0	4.321	1,653,346	1,647,288	0.37
	12	10	12.071	1,652,455	1,617,482	2.14
13	11	10	9.962	1,582,966	1,569,538	0.85
	36	35	19.288	1,633,910	1,600,539	9.07
14	16	16	31.305	1,645,474	1,588,868	3.44
	32	32	47.809	1,642,338	1,508,643	8.14
15	70	40	63.266	1,655,982	1,494,469	11.56
	35	5	46.657	1,647,567	1,545,999	6.53
16	23	23	7.188	1,651,444	1,521,539	7.87
	23	23	5.289	1,658,746	1,600,962	4.35
17	25	15	50.581	1,617,864	1,541,049	5.10
	72	60	59.602	1,618,755	1,514,712	6.58
18	218	0	42.182	1,597,971	1,119,919	31.12
	306	88	102.167	1,618,051	1,093,701	40.07
SD	85	43	35.448	30,559	189,708	11.74
Mean	87	25	37.240	1,625,375	1,427,987	13.30

SD = standard deviation

Table 7: Recombination information for each isolate in each *C. jejuni* pair considered for rate calibration

Pair no.	Rec blocks from root of subtree	Rec blocks from last common ancestor	r/m	Genome length (bp)	Bases in clonal frame (bp)	% of recombined genome
1	1	0	6.389	1,639,229	1,627,395	0.72
	1	0	6.389	1,634,719	1,622,885	0.72
2	6	6	3.042	1,618,681	1,606,663	0.74
	0	0	0.000	1,618,074	1,618,074	0.00
3	4	0	3.378	1,632,540	1,623,184	0.63
	5	1	0.058	1,626,877	1,618,438	0.66
4	1	0	6.389	1,635,771	1,623,937	0.72
	1	0	6.389	1,597,308	1,585,474	0.74
5	14	14	9.837	1,637,250	1,630,577	2.00
	2	2	2.247	1,639,143	1,637,492	0.10
6	23	23	2.992	1,622,009	1,610,144	1.73
	5	5	0.191	1,613,353	1,602,784	0.66
7	0	0	0.000	1,565,731	1,565,731	0.00
	4	4	0.502	1,605,399	1,576,627	1.79
8	6	6	1.295	1,605,876	1,587,041	1.17
	16	16	1.765	1,602,144	1,595,123	1.62
9	0	0	0.000	1,624,255	1,618,823	1.66
	2	2	0.594	1,635,479	1,630,084	0.33
10	0	0	0.000	1,638,978	1,638,978	0.00
	9	9	2.581	1,617,064	1,597,375	1.34
11	0	0	0.000	1,637,286	1,637,286	0.00
	1	1	0.070	1,634,549	1,633,954	0.04
12	14	5	3.102	1,631,249	1,569,740	3.77
	11	2	1.059	1,635,689	1,595,743	2.45
13	5	5	5.282	1,624,931	1,600,666	1.49
	0	0	0.000	1,635,860	1,635,860	0.00
14	11	3	7.825	1,531,436	1,515,728	1.03
	11	3	8.203	1,479,611	1,464,823	1.01
15	37	12	11.074	1,577,196	1,503,167	5.23
	27	2	4.535	1,578,646	1,527,929	3.21
16	13	5	3.493	1,629,646	1,594,397	3.68
	8	0	2.246	1,585,000	1,559,014	2.55
17	11	11	4.135	1,622,264	1,614,837	0.46
	0	0	0.000	1,608,872	1,608,872	0.00
18	3	3	0.442	1,589,659	1,585,982	0.23
	7	7	6.710	1,626,126	1,625,934	1.05
19	22	11	13.058	1,633,924	1,575,472	3.66
	28	17	10.982	1,571,410	1,495,992	5.30
20	8	8	32.016	1,529,278	1,290,989	18.64
	49	19	35.641	1,600,590	1,336,645	17.51
SD	11	6	7.585	35,024	74,747	3.94
Mean	9	5	5.098	1,609,328	1,579,746	2.22

SD = standard deviation

Table 8: *C. coli* "birthday problem" data and estimates of coalescence across sample time frame

Time cut-off (*t*)	No. of NCs in time (*st*)	No. of pairs < st (X)	Effective lineages (Z)
1	77	8	22,575
2	155	12	15,050
3	232	16	11,288
4	309	21	8,600
5	386	27	6,689
6	464	33	5,473
7	541	41	4,405
8	618	57	3,168
9	696	60	3,010
10	773	64	2,822
11	850	68	2,656
12	928	71	2,544
13	1,005	76	2,376
14	1,082	84	2,150
15	1,159	88	2,052
16	1,237	92	1,963
17	1,314	94	1,921
18	1,391	102	1,771
19	1,469	107	1,688
20	1,546	108	1,672
21	1,623	112	1,613
22	1,700	115	1,570
23	1,778	117	1,544
24	1,855	119	1,518
25	1,932	123	1,468
26	2,010	124	1,456
27	2,087	128	1,411
28	2,164	130	1,389
29	2,241	133	1,358
30	2,319	134	1,348
31	2,396	136	1,328
32	2,473	139	1,299
33	2,551	140	1,290
34	2,628	140	1,290
35	2,705	142	1,272
36	2,783	142	1,272
37	2,860	143	1,263
			mut + rec NCs/yr rate for *C. coli* = 77.3
			Y (all potential pairs) = 180,600

X = possible pairs; Y = potential pairs; Z = Coalescences ("birthdays")

Table 9: *C. jejuni* "birthday problem" data and estimates of coalescence across sample time frame

Time cut-off (*t*)	No. of NCs in time (*st*)	No. of pairs < st (X)	Effective lineages (Z)
1	14	76	21,888
2	28	129	12,895
3	42	150	11,090
4	56	163	10,205
5	71	174	9,560
6	85	182	9,140
7	99	190	8,755
8	113	194	8,575
9	127	198	8,401
10	141	209	7,959
11	155	215	7,737
12	169	221	7,527
13	183	225	7,393
14	197	230	7,233
15	212	237	7,019
16	226	242	6,874
17	240	249	6,681
18	254	254	6,549
19	268	256	6,498
20	282	258	6,448
21	296	262	6,349
22	310	267	6,230
23	324	270	6,161
24	338	276	6,027
25	353	278	5,984
26	367	281	5,920
27	381	287	5,796
28	395	292	5,697
29	409	295	5,639
30	423	300	5,545
31	437	303	5,490
32	451	310	5,366
33	465	312	5,332
34	479	314	5,298
35	494	318	5,231
36	508	320	5,198
37	522	324	5,134
38	536	329	5,056
39	550	333	4,995
40	564	335	4,966
41	578	340	4,893
42	592	341	4,878
43	606	342	4,864
44	620	344	4,836
45	635	349	4,766
46	649	352	4,726
			mut + rec NCs/yr rate for *C. jejuni* = 14.1
			Y (all potential pairs) = 1,663,488

X = possible pairs; Y = potential pairs; Z = Coalescences ("birthdays")

Fig 1.

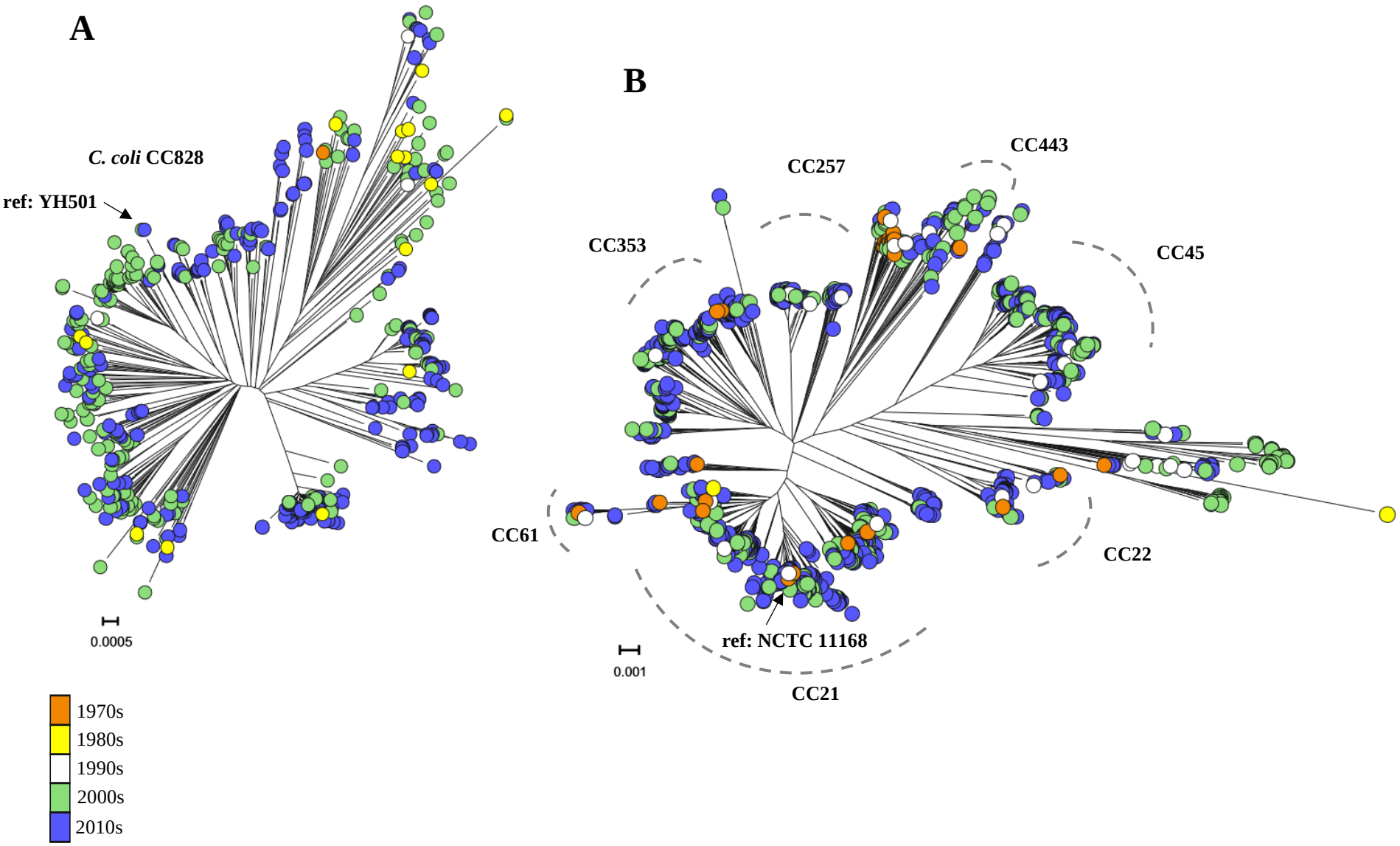
A
C. coli CC828
ref: YH501
0.0005
B
CC257
CC443
CC353
CC45
CC61
CC22
ref: NCTC 11168
0.001
CC21
1970s
1980s
1990s
2000s
2010s

Fig 2.

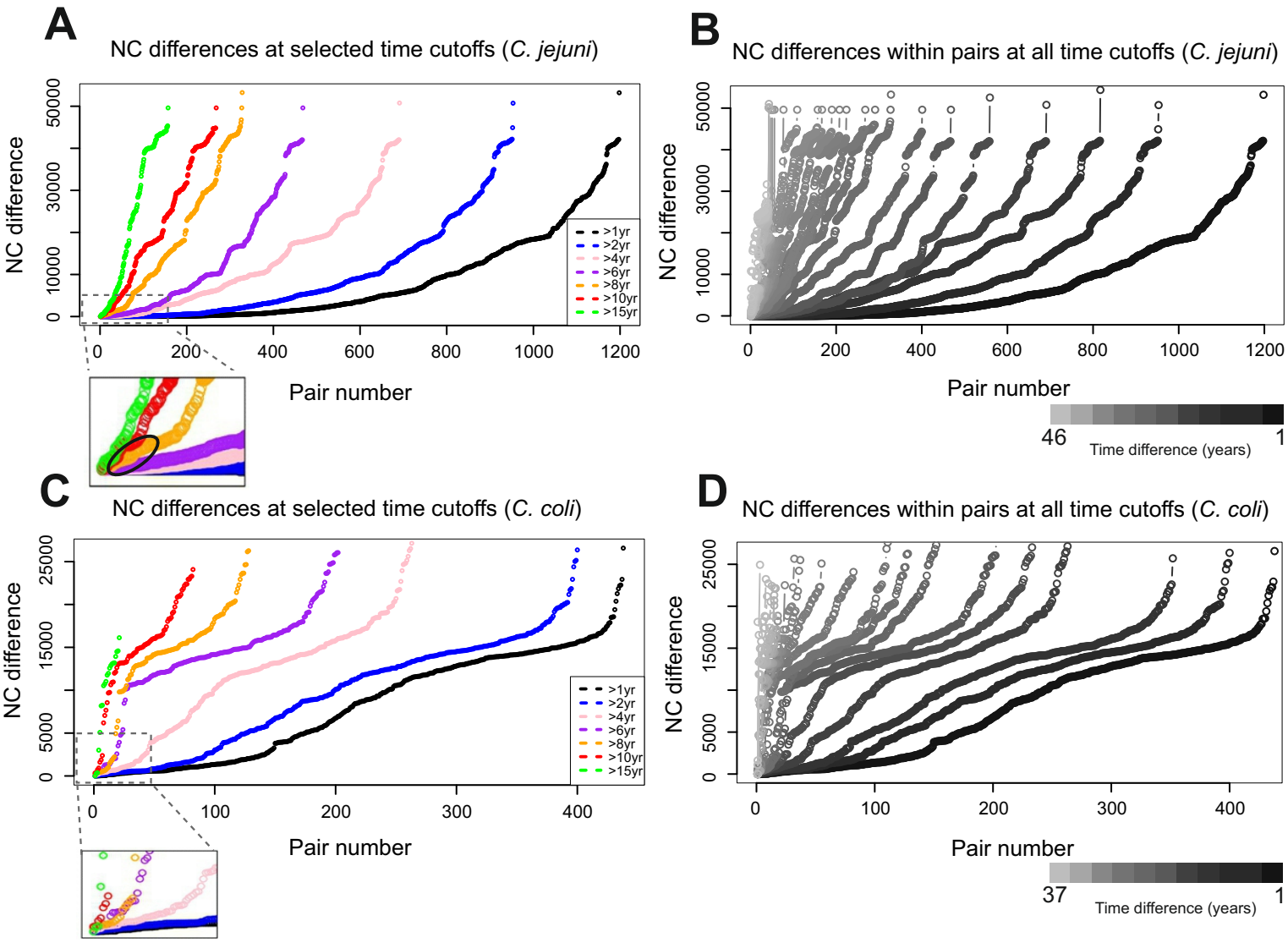
A
NC differences at selected time cutoffs (C. jejuni)
NC difference
Pair number
>1yr
>2yr
>4yr
>6yr
>8yr
>10yr
>15yr
B
NC differences within pairs at all time cutoffs (C. jejuni)
NC difference
Pair number
46
1
Time difference (years)
C
NC differences at selected time cutoffs (C. coli)
NC difference
Pair number
>1yr
>2yr
>4yr
>6yr
>8yr
>10yr
>15yr
D
NC differences within pairs at all time cutoffs (C. coli)
NC difference
Pair number
37
1
Time difference (years)

Fig 3.

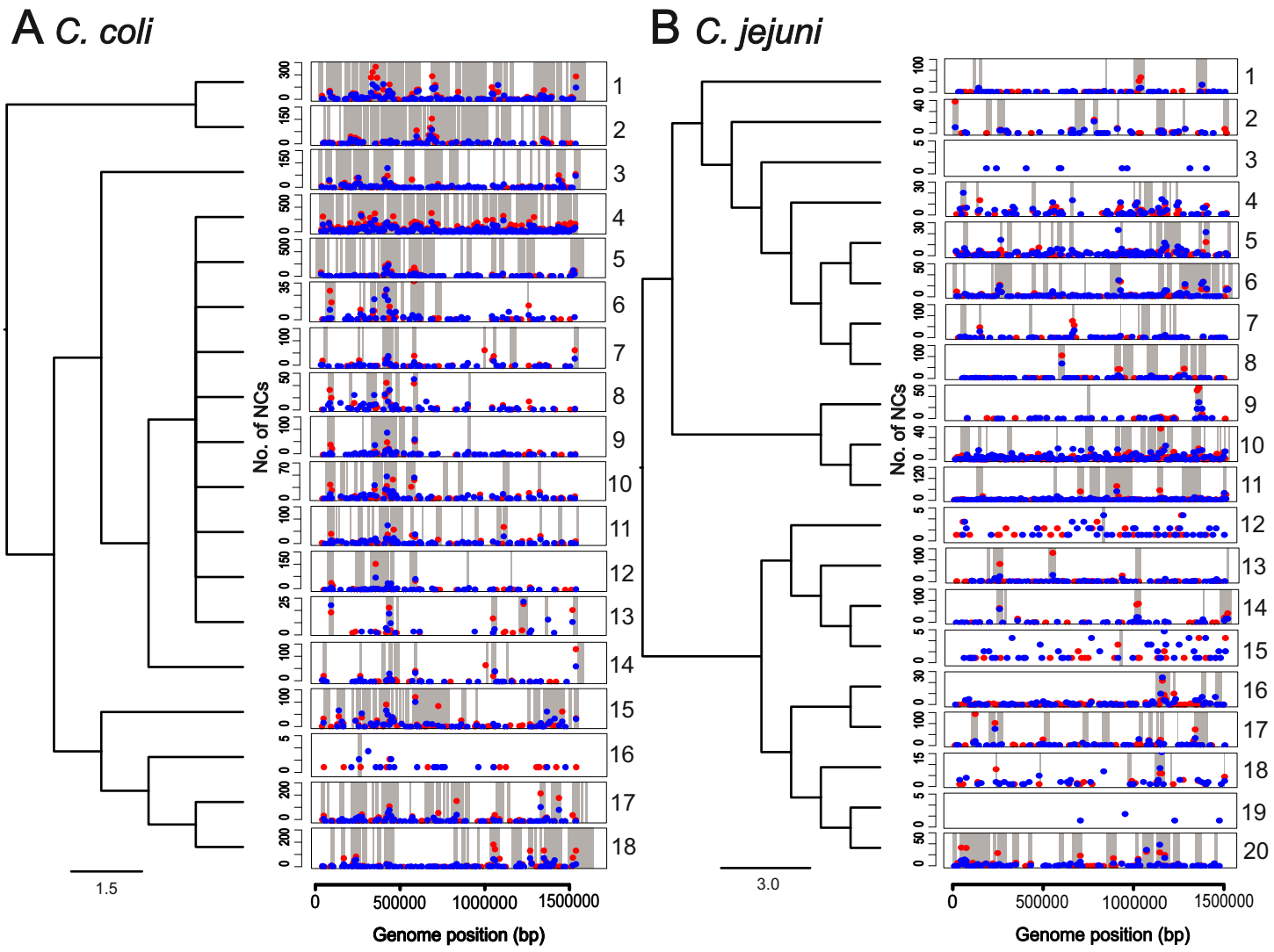
A C. coli
B C. jejuni
No. of NCs
Genome position (bp)
0
500000
1000000
1500000
1.5
3.0

Fig 4.

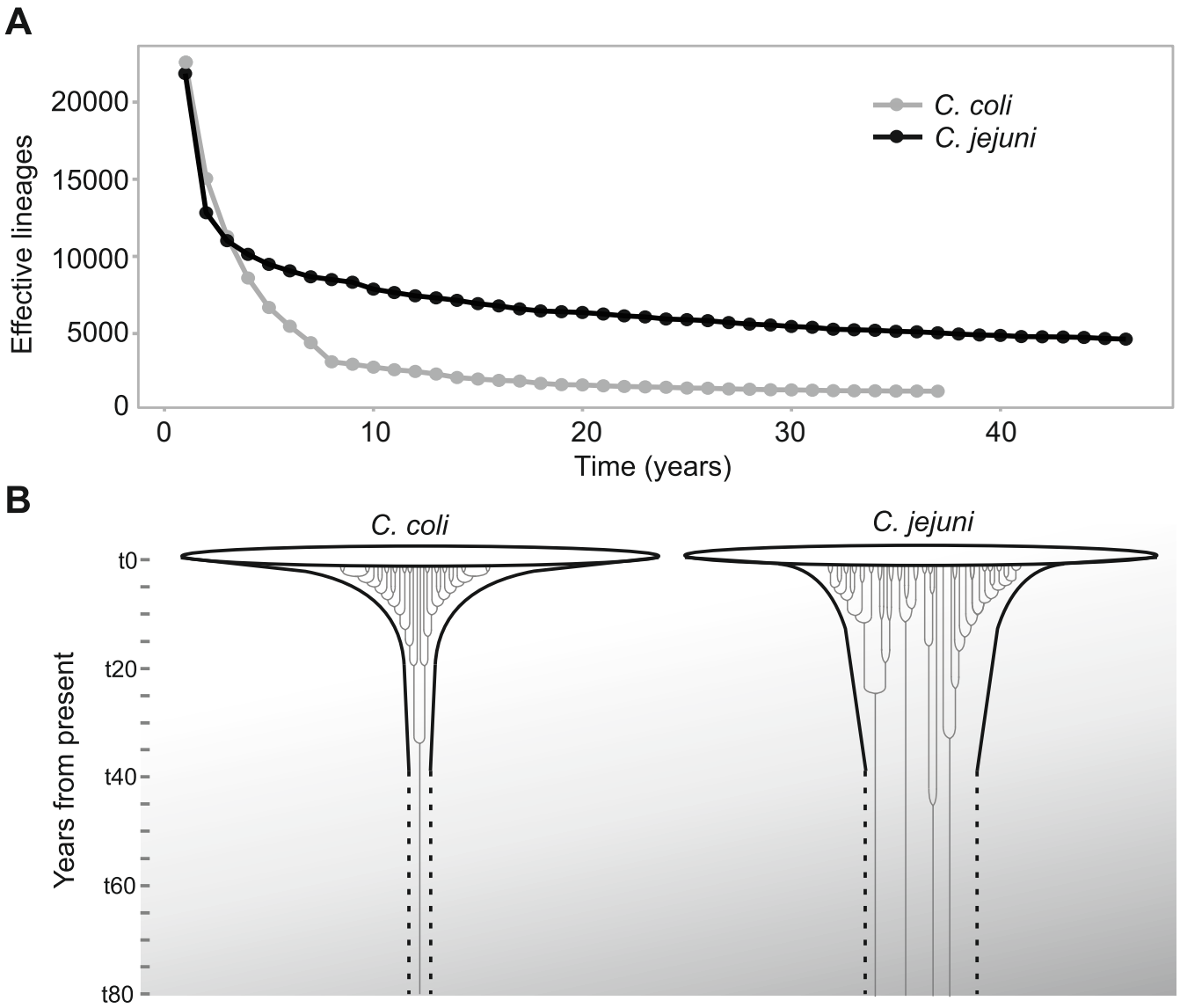
A
Effective lineages
20000
15000
10000
5000
0
0
10
20
30
40
Time (years)
C. coli
C. jejuni
B
C. coli
C. jejuni
Years from present
t0
t20
t40
t60
t80

S1 Figure.

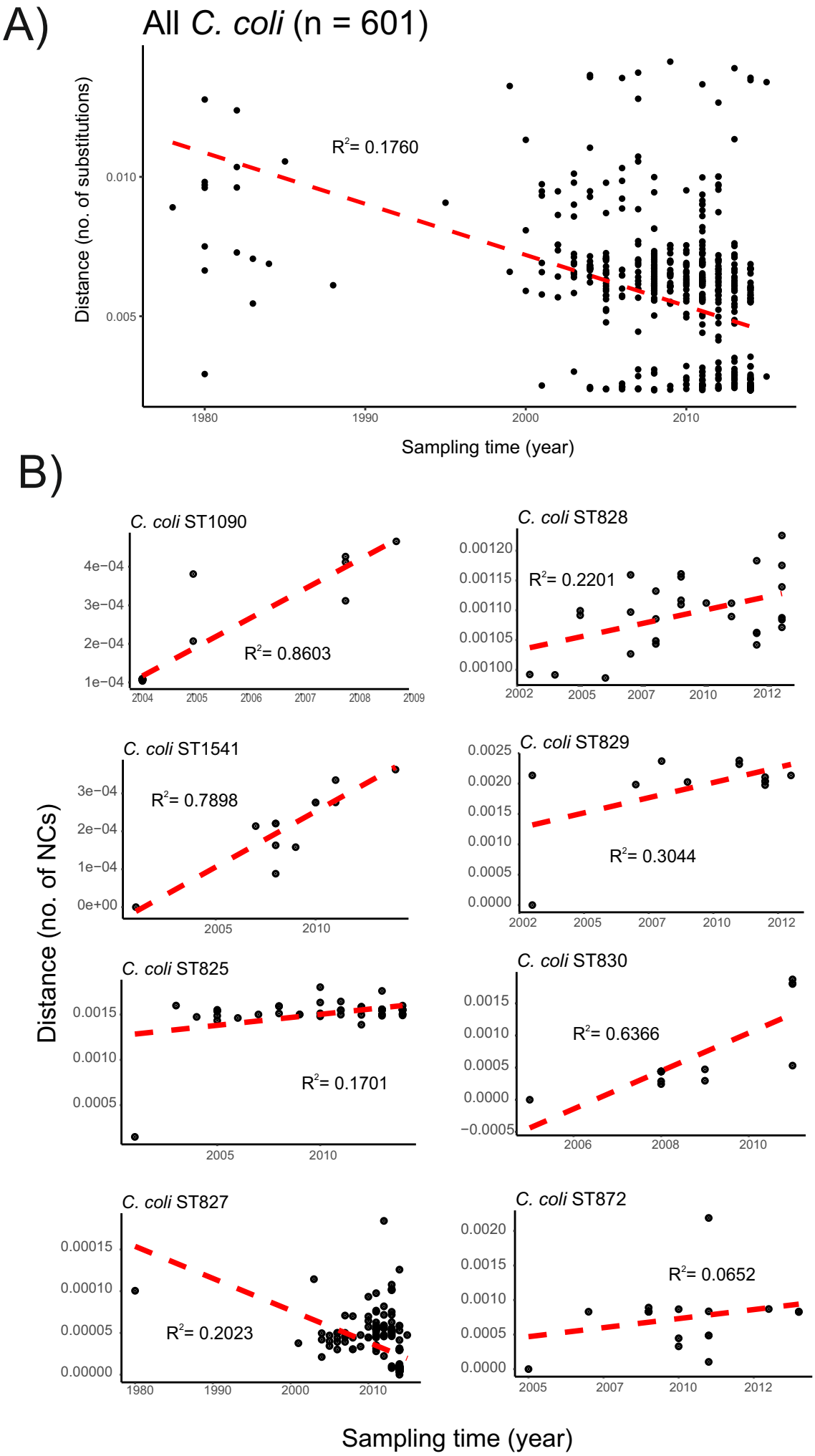
A)
All C. coli (n = 601)
Distance (no. of substitutions)
R²= 0.1760
0.010
0.005
1980
1990
2000
2010
Sampling time (year)
B)
C. coli ST1090
R²= 0.8603
C. coli ST828
R²= 0.2201
C. coli ST1541
R²= 0.7898
C. coli ST829
R²= 0.3044
C. coli ST825
R²= 0.1701
C. coli ST830
R²= 0.6366
C. coli ST827
R²= 0.2023
C. coli ST872
R²= 0.0652
Distance (no. of NCs)
Sampling time (year)

S2 Fig.

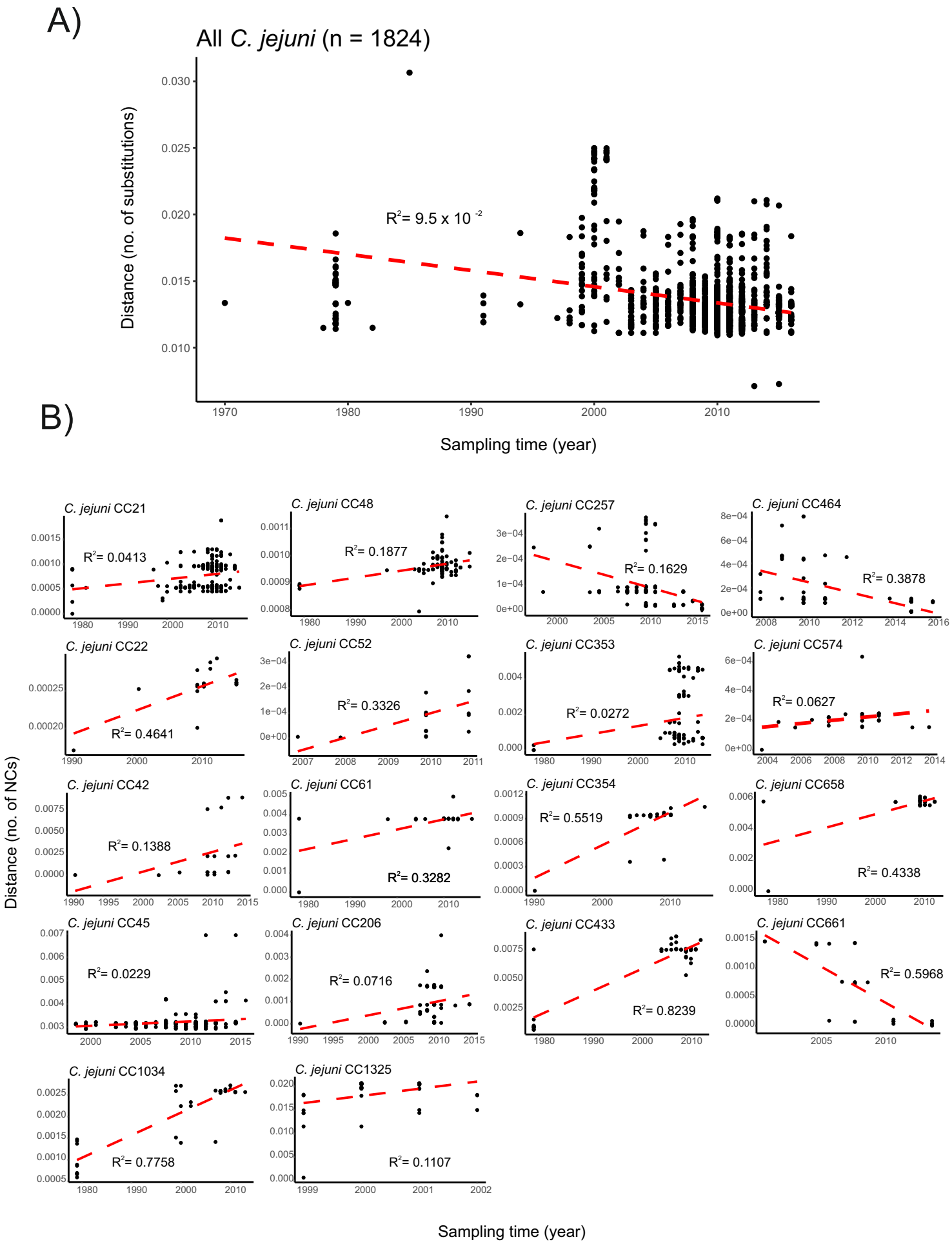
A)
All C. jejuni (n = 1824)
Distance (no. of substitutions)
R²= 9.5 x 10 -2
Sampling time (year)
B)
C. jejuni CC21
R²= 0.0413
C. jejuni CC48
R²= 0.1877
C. jejuni CC257
R²= 0.1629
C. jejuni CC464
R²= 0.3878
C. jejuni CC22
R²= 0.4641
C. jejuni CC52
R²= 0.3326
C. jejuni CC353
R²= 0.0272
C. jejuni CC574
R²= 0.0627
C. jejuni CC42
R²= 0.1388
C. jejuni CC61
R²= 0.3282
C. jejuni CC354
R²= 0.5519
C. jejuni CC658
R²= 0.4338
C. jejuni CC45
R²= 0.0229
C. jejuni CC206
R²= 0.0716
C. jejuni CC433
R²= 0.8239
C. jejuni CC661
R²= 0.5968
C. jejuni CC1034
R²= 0.7758
C. jejuni CC1325
R²= 0.1107
Distance (no. of NCs)
Sampling time (year)

S3 Fig.

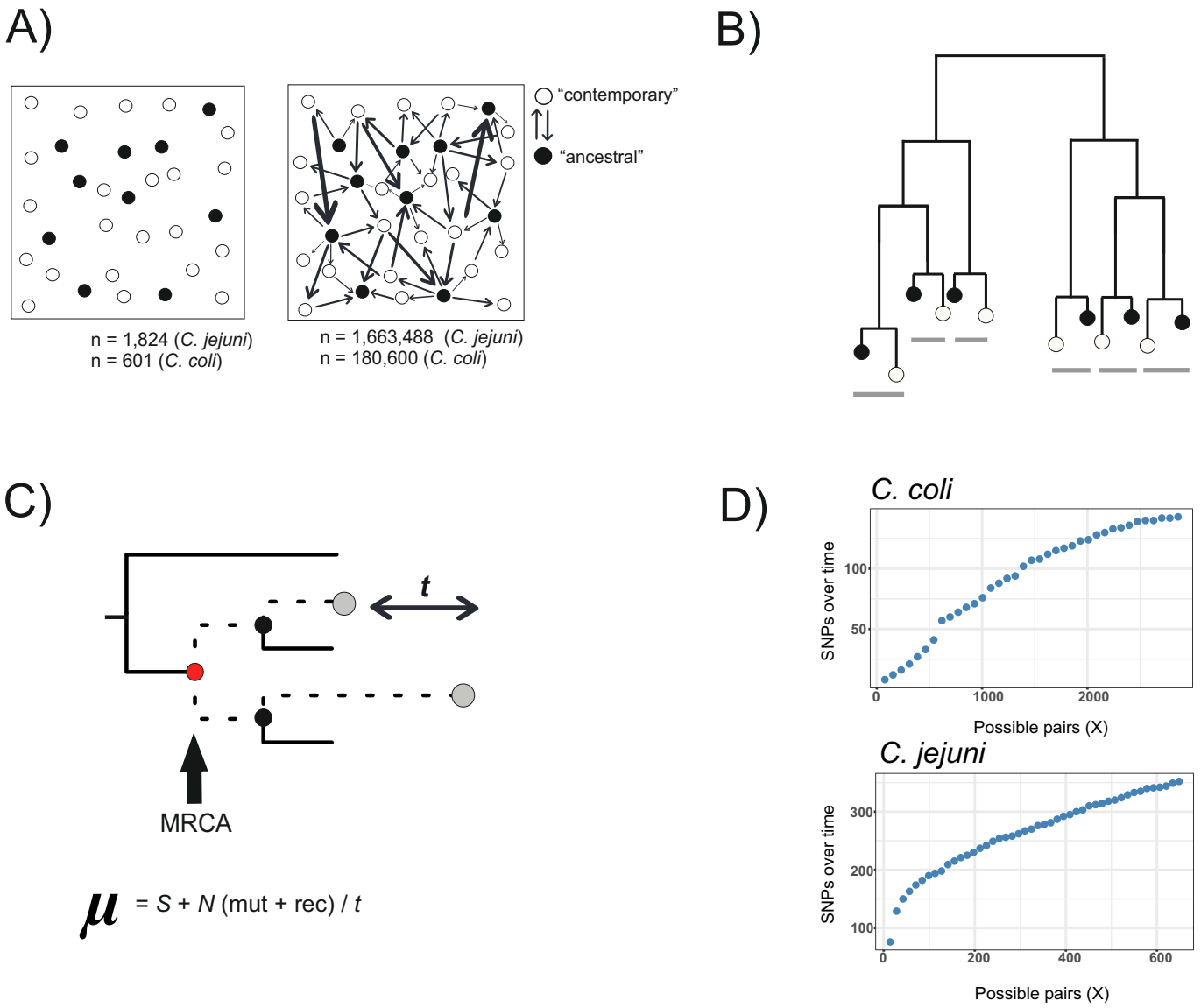
A)
n = 1,824 (C. jejuni)
n = 601 (C. coli)
n = 1,663,488 (C. jejuni)
n = 180,600 (C. coli)
"contemporary"
"ancestral"
B)
C)
t
MRCA
μ = S + N (mut + rec) / t
D)
C. coli
SNPs over time
Possible pairs (X)
C. jejuni
SNPs over time
Possible pairs (X)